ACS OMEGA

http://pubs.acs.org/journal/acsodf

Article

Copper Complexes of 1,4-Naphthoquinone Containing Thiosemicarbazide and Triphenylphosphine Oxide Moieties; Synthesis and Identification by NMR, IR, Mass, UV Spectra, and DFT Calculations

Mohammed B. Alshammari, Ashraf A. Aly,* Stefan Bräse,* Martin Nieger, Mahmoud A. A. Ibrahim, and Lamiaa E. Abd El-Haleem

Cite This: *ACS Omega* 2022, 7, 34463−34475

Read Online

ACCESS | Metrics & More | Article Recommendations | Supporting Information

ABSTRACT: New 1,4-naphthoquinone derived by triphenylphosphaneylidene (Ph_3P) and *N*-substituted-hydrazine-1-carbothioamides were obtained during a one-pot reaction of 2,3-dichloro-1,4-naphthoquinone with thiosemicarbazides, Ph_3P and in the presence of triethyl amine (Et_3N) as a catalyst. The structure of the ligands was established by ESI, IR, and NMR spectra, in addition to elemental analyses and X-ray structure analysis. On subjecting the newly prepared ligands with $CuCl_2$ and Ph_3P, autoxidation occurs, and (*E*)-(2-(1,4-dioxo-3-(triphenyl phosphanylidene)-3,4-dihydronaphthalen-2(1*H*)-ylidene)carbamothioyl)-hydrazinyl)-((triphenylphosphanyl)oxy)copper derivatives were formed in very good yields. The structure of the obtained complexes was proved by ESI, IR, NMR, and UV spectra, in addition to elemental analyses and theoretical calculations.

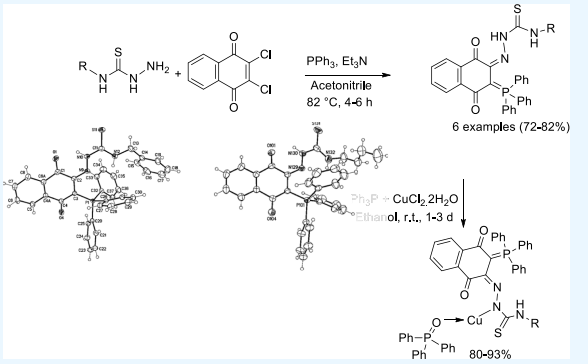

1. INTRODUCTION

Natural hydroxy derivatives of 1,4-naphthoquinone lawsone and juglone with hydroxyl groups in the α- and β-positions of the naphthalene core form salts and complexes with cations of various metals and are used as dyes.[1] Protein binding, DNA binding/cleavage, and in vitro cytotoxicity studies of 2-((3-(dimethylamino)-propyl)amino)naphthalene-1,4-dione and its four coordinated M(II) complexes [M(II) = Co(II), Cu(II), Ni(II), and Zn(II)] have been investigated. The complexes demonstrated a comparable *in vitro* cytotoxic activity against two human cancer cell lines (MCF-7 and A-549) with cisplatin. AO/EB and DAPI staining studies suggest an apoptotic mode of cell death in these cancer cells, with the compounds under investigation.[2] A series of nine Ru^{II} arene complexes bearing tridentate naphthoquinone-based *N*,*O*,*O*-ligands were synthesized and characterized. The cytotoxic profile exhibited much higher cytotoxicity in SW480 colon cancer cells than in the broad chemo- (incl. platinum-) sensitive CH1/PA-1 teratocarcinoma cells. This activity pattern, reduced or slightly enhanced ROS generation, and the lack of DNA interactions indicate a mode of action different from established or previously investigated classes of metallodrugs.[3]

The reactions of 1,4-naphthoquinone with triphenylphosphine (Ph_3P) have been previously described. As, for example, in the reaction of fluoronaphthoquinone (**1**) with triphenylphosphine (Ph_3P), derivatives of phosphonium betaines derived from hexafluoro-1,4-naphthoquinone: (triphenyl-[5,6,7,8-tetrafluoro-1-oxido-4-oxo-3-(phenylimino)-3,4-dihydro-naphthalen-2-yl]phosphonium) **3** (Scheme 1), were obtained.[4] The reaction was explained as due to the formation of intermediate **2** (Scheme 1). Depending upon reaction conditions, it was reported that Ph_3P reacted with *p*-chloranil (**4**) to produce either Zwitter salts **5** or **6**[5] (Scheme 1). However, in aqueous alcoholic medium, 3-(triphenylphosphoranylidene)naphthalene-1,2,4(3*H*)-trione (**8**)[6] was obtained from the reaction of 2,3-dichloro-1,4-naphthoquinone (**7**) with Ph_3P (Scheme 1).

In the same manner, bisphosphonium salt containing a 1,4-dihydroxynaphthyl-substituted moiety was synthesized in high yield by the reaction of 2-methyl-1,4-naphthoquinone with three equivalents of Ph_3P and hydrogen bromide.[7] Metal-free synthesis of aryltriphenylphosphonium bromides by the reaction of Ph_3P with aryl bromides in refluxing phenol was developed.[8] With the high reactivity of naphthoquinones, 2,3-

Received: June 30, 2022
Accepted: August 29, 2022
Published: September 16, 2022

Scheme 1. Effect of Ph_3P on Halogenated Naphthoquinones 1, 4, and 7

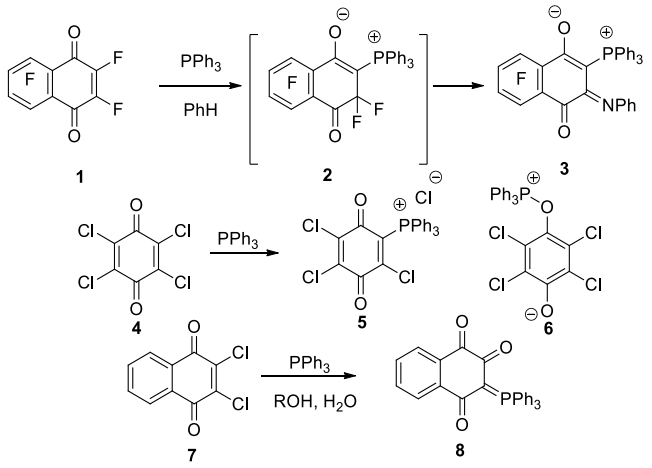

dichloro-1,4-naphthoquinone (DCHNQ, **7**) reacted with nucleophiles and substituted one or both chlorine atoms.[9−13] It was found that the reaction of **7** with *p*-nitrobenzhydrazide (**9**) in 1:2 or 2:l ratio in DMF gave only the disubstituted product, bis-(-*p*-nitrobenzhydrazino)-1,4-naphthoquinone (**10**). However, when an ethanolic solution of **7** and **9** was refluxed for 21 h, the main product was a bright red precipitate of **11**[14] (Scheme 2).

Scheme 2. Nucleophilic Addition of Aroylhydrazide 9 to Compound 7

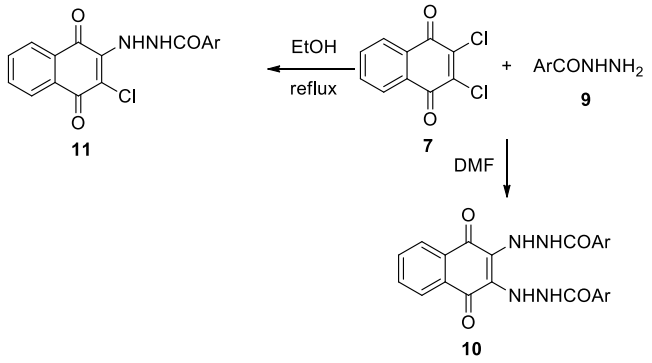

On the basis that triphenylphosphine oxide ($Ph_3P{=}O$) can form facile complexes with some metal salts, Hergueta et al.[15] reported the facile removal by complexation with $CaBr_2$, with $Ph_3P{=}O$ in ethereal solvents or toluene. The resulting insoluble precipitated complex was easily eliminated from crude reaction mixtures in high yields by filtration without the need for purification by column chromatography.[15]

Copper(I) and silver(I) chloride complexes containing PPh_3 and 4-phenyl-thiosemicarbazide (4-PTSC) ligands were prepared and structurally analyzed, namely, $[CuCl(4\text{-PTSC})(PPh_3)_2]$ (**12**) and $[AgCl(4\text{-PTSC})(PPh_3)_2]CH_3CN$. Both compounds exhibit a distorted tetrahedral metal coordination environment with two P atoms from two PPh_3 ligands, one terminal S atom from the 4-PTSC ligand, and a chloride ion (Figure 1).[16]

The reactions between $[CuCl_2(PPh_3)_2]$ and 3,3-diphenyl-1-(2,4-dichlorobenzoyl)thiourea, 3,3-diisobutyl-1-(2,4-dichlorobenzoyl)thiourea, or 3,3-diethyl-1-(2,4-dichlorobenzoyl)thiourea in benzene gave four-coordinated tetrahedral copper(I) complexes of the type $[CuCl(HL)(PPh_3)_2]$ [HL = 3,3-dialkyl/aryl-1-(2,4-dichlorobenzoyl)-thiourea derivatives].[17]

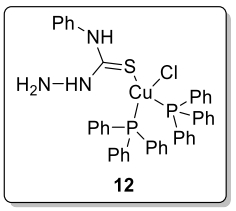

Figure 1. Copper(I) chloride complex containing PPh_3 and 4-phenylthiosemicarbazide (4-PTSC) ligand **12**.

Previously, we reacted thiosemicarbazones derived from 2-quinolone with Cu(I), Cu(II), and Ni(II) salts.[18] Monodentate Cu(I) quinoloyl-substituted ligands were observed, whereas Ni(II) and Cu(II) gave bidentate-thiosemicarbazone derived by 2-quinolones. Subsequently, molecular docking was used to evaluate each analog's binding affinity and the inhibition constant (k_i) to the RdRp complex of SARS-CoV-2.[18] We also synthesized a series of paracyclophane-substituted thiosemicarbazones, thiocarbazones, hydrazones, and thioureas to study their complexation capability toward copper (I) and Cu (II) salts. Tridentate and bidentate of the aforesaid paracyclophane-substituted ligands were observed. Thiosemicarbazonyl, hydrazonyl, and thiourea paracyclophane derivatives formed with Cu(I) and Cu(II) salt tridentate and bidentate structures, whereas no complexes were observed for the prepared thiocarbazone derivatives.[19]

Copper complexes have numerous properties, including proteasome activity inhibitors,[20] DNA intercalation,[21] and anticancer chelators. They can also increase the activity of the ligand itself. For example, 4-cyclohexyl-3-(4-nitrophenyl)-methyl-1,2,4-triazolin-5-thione has no activity against some selected bacteria, but after obtaining the metal(II) complex, the activity increases to a mild score.[22]

From this, we here aim to investigate the reaction of 2,3-dichloro-1,4-naphthoquinone (**7**) together with thiosemicarbazides and Ph_3P to achieve the expected bi-nucleophilic substituted naphthoquinone. The newly obtained triphenylphosphine-ylidene-3,4-dihydronaphthalen-2(1*H*)-ylidene)-*N*-substituted-hydrazine-1-carbothioamides were then subjected to complexation toward $CuCl_2$ and Ph_3P. The stability of these complexes was discussed using a plethora of quantum mechanical calculations and by executing Hirshfeld surface (HS) analysis.

2. RESULTS AND DISCUSSION

Thiosemicarbazides **14a-f** were prepared by reacting substituted isothiocyanates **13a-f** with hydrazine in ethanol as a solvent.[23] Upon mixing equimolar amounts of **14a-f** with 2,3-dichloro-1,4-naphthoquinone (**7**), Ph_3P, and in the presence of Et_3N as a catalyst and acetonitrile as a solvent, triphenylphosphine-ylidene(-3,4-dihydronaphthalen-2(1*H*)-ylidene)-*N*-substituted-hydrazine-1-carbothioamides **15a-f** were obtained in 72−82% yield (Scheme 3).

The mass spectrum of compound **15c** revealed $[M + H]^+$ at m/z = 598 (75), whereas the molecular ion peak at m/z = 597 (30). HRMS FAB mass confirmed the molecular formula of **15c** $C_{36}H_{29}N_3O_2P_1{}^{32}S_1$, $[M + H]^+$) calcd: 598.1718; found: 598.1717. The ^1H NMR spectrum displayed the two NH

https://doi.org/10.1021/acsomega.2c04113
ACS Omega 2022, 7, 34463−34475

Scheme 3. Synthesis of Ligands 15a-f

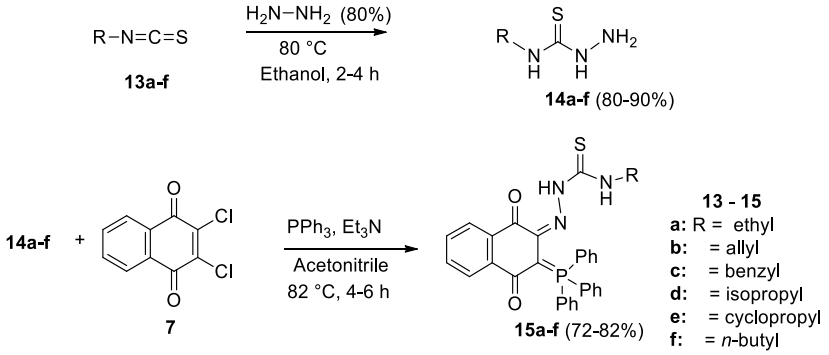

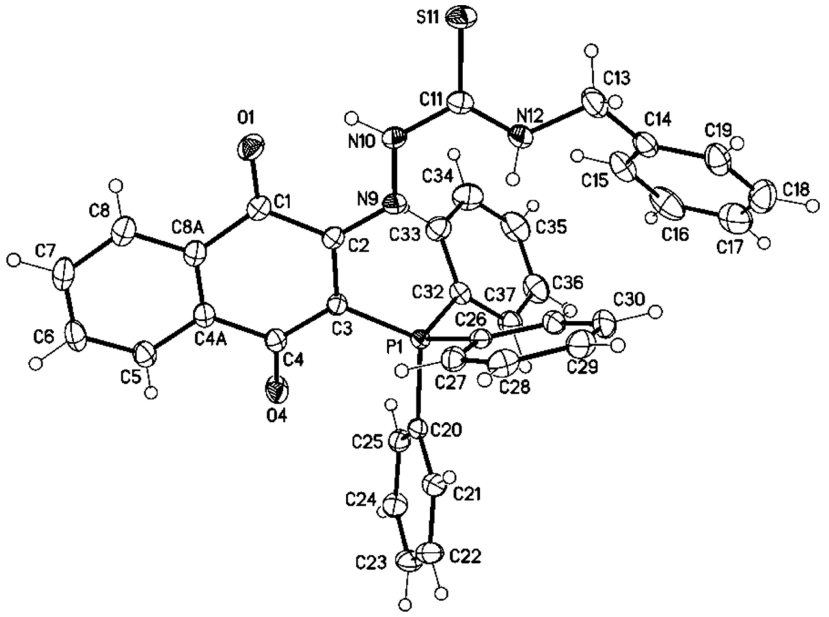

Figure 2. Molecular structure of compound **15c** (displacement parameters are drawn at 50% probability level). Selected bond distances [Å] and angles [°]: C2−N9 1.3088(16), N9−N10 1.3674(14), N10−C11 1.3546(17), C11−S11 1.6775(13), C11−N12 1.3297(17), N12−C13 1.4557(17); C2−N9 N10 119.45(10), N9−N10−C11 119.65(10), N10−C11−S11 119.43(10), N10−C11−N12116.90(11), C11−N12−C13 122.64(11).

protons at δ_H = 13.04 (s, 1H, NH^1) and at 6.85 (s, 1H, NH^2). The benzyl-CH_2 resonated as a multiplet, in the ^{1}H NMR spectrum, at δ_H = 4.38−4.20. The ^{13}C NMR spectrum showed the carbonyl carbon signals at δ_C = 177.2 and 176.3, whereas the C═S and benzylic-CH_2 carbon signals appeared at δ_C = 162.8 and 46.9 ppm, respectively. IR spectroscopy revealed the NH-stretching, C═P, and C═S groups at $\tilde{\nu}$ = 3340−3055, 1153, and 988 cm^{-1}, respectively. X-ray structure analysis confirmed the structure of **15c,** as shown in Figure 2.

Mass spectroscopy of **15f** revealed $[M + H]^+$at m/z = 564 (100), whereas the molecular ion peak appeared at m/z = 563 (30%). HRMS confirmed $[M + H]^+$ of compound **15f** as $C_{33}H_{31}N_3O_2P_1{}^{32}S_1$. The ^{1}H NMR spectrum showed the two NH protons at δ_H = 13.18 and 6.74. In the ^{1}H NMR spectrum, the butyl protons resonated as a double-doublet (J = 7.7, 1.5 Hz, 2H) and three multiplets at δ_H = 3.58, 1.60−1.49, 1.35−1.26, and 1.02−0.99 ppm, respectively. The ^{13}C NMR spectrum showed the carbonyl carbon signals at δ_C = 186.1 and 185.9, whereas C=S resonated at 178.4 ppm. The butyl carbon signals resonated in the ^{13}C NMR spectrum at δ_C = 44.6, 30.4, 20.1, and 14.0 ppm. IR spectroscopy displayed the NH-stretching at $\tilde{\nu}$ = 3340−3053 (w, NH), whereas the two carbonyl groups and C═N appeared at $\tilde{\nu}$ = 1586, 1521, and 1434, respectively. Besides, the C═P and the C═S groups appeared as strong bands in the IR spectra at $\tilde{\nu}$ = 1170 and 992 cm^{-1}, respectively. The structure of **15f** was confirmed by X-ray structural analysis, as shown in Figure 3.

In the crystal structures of **15c** and **15f,** are the bond distances and angles in the expected range with a slight delocalization of the π-electron in the thiosemicarbazide moiety (see cif-file). The thiosemicarbazide and 1,4-naphthoquinone moieties are coplanar.

The mechanism describes that the formation of **15a-f** is based upon the addition of Ph_3P to C-1 (or C-2) in **7** to give the Zwitterion **17**, which would be in resonance with the intermediate **18** (Scheme 4). The addition of **14a-f** in the presence of Et_3N would then accompany the elimination of a molecule of HCl and another of Ph_3P to give **19a-f** (Scheme 4). Subsequently, the extruded Ph_3P would again add to halogenated intermediates **19a-f** to produce salts **20a-f** (Scheme 4). Finally, a molecule of Et_3N would facilitate the formation of **20a-f** *via* the elimination of a molecule of triethylammonium hydrochloride.

https://doi.org/10.1021/acsomega.2c04113
ACS Omega 2022, 7, 34463−34475

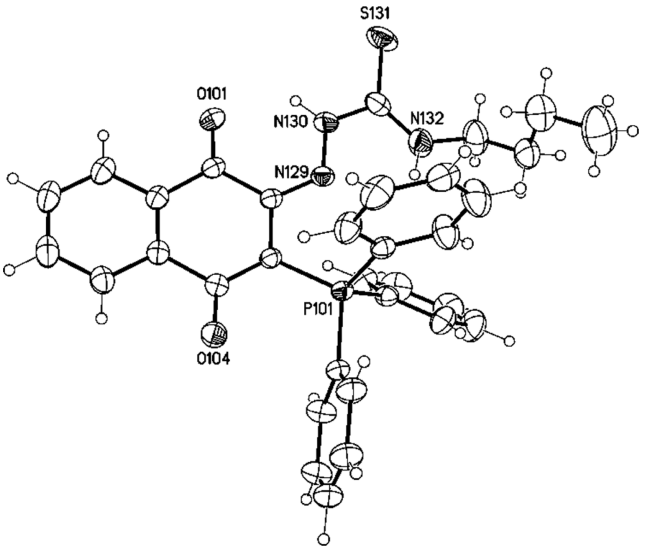

Figure 3. Molecular structure of one crystallographic independent molecule (with *n*-butyl substituent) of compound **15f** (displacement parameters are drawn at a 30% probability level). Selected bond distances [Å] and angles [°]: C102−N129 1.303(3), N129−N130 1.363(3), N130−C131 1.364(4), C131−S131 1.671(3), C131−N132 1.337(5), N132−C133 1.457(4); C102−N129 N130 120.4(2), N129−N130−C131 119.4(3), N130−C131−S131 119.3(3), N130−C131−N132 115.3(3), C131−N132−C133 126.8(3).

Interestingly, the reaction of equal equivalents of compounds **15a-f** with Ph_3P and $CuCl_2{\cdot}2H_2O$ in ethanol at rt and for 1−3 d produced the Cu-complexes **16a-f** (Scheme 5). Based on IR, ^1H NMR, and mass spectra, together with elemental analysis, the NH-3 proton of the thiosemicarbazone moiety, in **15a-f**, was eliminated, and aerial oxidation occurred, as shown in Scheme 5.

Reagents and conditions: **15a-f** (1.00 equiv), $CuCl_2{\cdot}2H_2O$ (1.00 equiv) and Ph_3P (1.00 equiv) in absolute EtOH (40 mL), room temperature (2−4 h). Column chromatography (CC) using EtOAc/hexane (5:1).

2.1. Assignment of the Ligands 15a-f and Their Cu-Complexes 16a-f by Mass Spectroscopy and Elemental Analyses. The molecular formulae of the obtained complexes were proved according to the mass spectroscopic data and the elemental analyses. Physical data from the color, m.p., and yield in g (%) were illustrated, as shown in Table 1.

Elemental analyses and mass spectra indicated that the formed Cu(II)-complexes **16a-f** resulted in the sum of the molecular weight of compounds **15a-f** with one copper atom together with a Ph_3PO molecule. Elemental analyses of compounds **16a-f** are shown in Table 2.

2.2. Assignment by IR Spectra. The significant bands in infrared spectra for both ligands **15a-f** and their metal complexes **16a-f** are represented in Table 3. The symmetrical stretching of NH bands for compounds **16a-f** was absorbed in the region at their expected region of IR spectra. The shift in functional groups from the ligands to the corresponding complexes supported the chelating process. Coordination occurred *via* N-2 and the oxygen atom of Ph_3P. The C═S stretching gave slight shifts in the case of a comparison between **15a-f** and **16a-f**. Most indicative is the new appearance of P═O, Cu−N, and Cu−O bands during the comparison between **15a-f** and **16a-f**. For example, IR spectroscopy of **15a** showed the following bands at ν = 3345, 3052 for NH stretching, 1188 (as a strong band) for C═P, and 993 (as a strong band) cm^{-1} for s, C═S. In the case of **16a**, the NH stretching was absorbed as a weak band at ν = 3054, whereas at ν = 1178, as a strong band for the C═P group. New bands were noted at ν = 1019 (m, P=O), 536 (s, Cu−N), and 457 cm^{-1} (s, Cu−O). Similar values of the previous three groups were previously reported.[24,25] The same trend was also observed in all compounds **16b-f** (Table 2).

2.3. Assignment of the Complexes 16a-f by NMR Spectra. Together with the elemental analyses, mass, and IR spectra, the chemical shift in NMR spectra, indicating the complexation process of **15a-f** with Cu(II) to form **16a-f**, as shown in Table 4. As it is known that although most NMR measurements are conducted on diamagnetic compounds, paramagnetic samples are also amenable to analysis and give rise to special effects indicated by a wide chemical shift range and broadened signals.[26,27] However, several papers reported the use of the Cu(II) complex with Ph_3P of the composition $CuCl_2(PPh_3)_2$.[28−30] The previous studies showed that the oxidation state of II cannot be stabilized for copper in the presence of such a reducing ligand like Ph_3P. Therefore, Cu(II) is converted into Cu(I) during complexation with Ph_3P and compounds **15a-f**. We here note that NMR spectra could be distinguished, and there are remarkable shifts in some values of the chemical shifts (δ) of ^1H NMR and ^{13}C NMR spectra of compound **15a**, as an example, compared with its complex **16a**. In the ^1H NMR spectrum, NH-2 resonated at δ_H = 12.90, whereas NH-1 appeared at δ_H = 5.77. The ethyl protons appeared as a quartet at δ_H = 3.19 for CH_2^{ethyl}, whereas a triplet at δ_H = 0.62 ppm (J = 7.1 Hz). In the case of **16a** (Table 4), the ^1H NMR spectrum of only NH-1 at δ_H = 5.49, whereas N-2 didn't reveal any proton. The ethyl protons appeared as a quartet at δ_H = 4.05 (J = 7.1 Hz) and a triplet at δ_H = 1.20 ppm

Scheme 4. Mechanism Describes the Formation of Ligands 15a-f

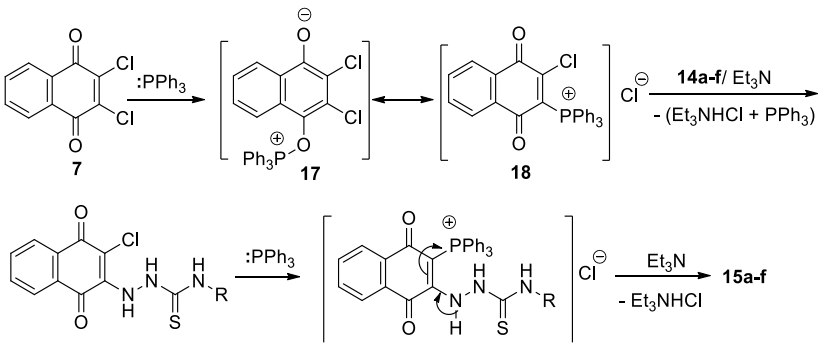

https://doi.org/10.1021/acsomega.2c04113
ACS Omega 2022, 7, 34463−34475

Scheme 5. Mechanism Describes the Formation of Cu-Complexes 16a-f

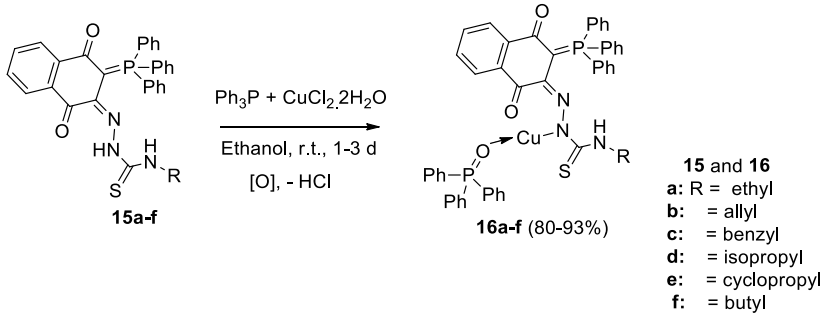

Table 1. Physical Data and Yield in g (%) of Complexes 16a-f

no	complex	color	mp (°C)	yield g (%)
1	**16a**	deep blue	250−252 (decomp)	0.718 (82)
2	**16b**	deep blue	244−246 (decomp)	0.745 (84)
3	**-16c**	deep blue	262−264 (decomp)	0.872 (93)
4	**-16d**	deep blue	268−270 (decomp)	0.712 (80)
5	**-16e**	deep blue	249−251 (decomp)	0.763 (86)
6	**16f**	deep blue	257−259 (decomp)	0.795 (90)

(J = 7.1 Hz). The ^{13}C NMR spectrum of **15a** showed the carbonyl carbon signals at δ_C = 183.7 and 183.6, whereas C═S resonated at δ_C = 176.7 ppm. The ethyl carbons appeared at δ_C = 37.9 for CH_2 and at δ_C = 13.5 ppm for CH_3 (as shown in the Supporting Information). In the case of **16a**, in the ^{13}C NMR spectrum, the carbonyl carbon signals resonated at δ_C = 186.0 and 183.6 ppm. (C_q, *C*O), whereas the C═S carbon signal appeared at δ_C = 175.4 ppm. The ethyl carbon signals resonated at δ_C = 39.0 (CH_2^{ethyl}) and 13.6 ppm (CH_3^{ethyl}). Significantly, the exocyclic carbon signal (in C═N) appeared in the ^{13}C NMR spectrum of **15a** at δ_C = 142.8, whereas for **16a**, it appeared at δ_C = 143.1.

2.4. UV−Vis Studies. UV−vis absorption spectra of the Cu(II) complexes **16a-f** were measured from 200 to 800 nm, using acetonitrile. The blue-colored compounds exhibited bands in UV−vis spectra, ranging from 540 to 548 nm (i.e., n−π*). These bands can be attributed to ligand-to-metal charge transfer transitions from nitrogen to Cu(II). N → Cu ← O bands are common in electronic spectra of metal complexes of thiosemicarbazides. Representative examples are the UV/vis spectra of compounds **16b** and **16c** (Figure 4). In the field of inorganic chemistry, UV/Vis spectra are usually associated with d−d transitions and colored transition metal complexes.

2.5. Optimized Geometries. To verify the experimental findings, the complexes under study were optimized and are illustrated in Figure 5. No imaginary frequencies were noticed for the optimized complexes, ensuring that the obtained geometries were true minima. The energy differences (ΔE) between the investigated complex (E) and the most stable one (E_1) are also given in Figure 5. The single point energies ensured the further favorability of complex **1** over other studied conformations.

2.6. HS Analysis. HS analysis was considered a dependable technique to qualitatively elucidate intermolecular interactions within crystal structures and unveil the interactions around the molecules' surface.[31−34] HSs, including the d_{norm} and its associated 2D fingerprints, shape index, and curvedness, were mapped for the studied complexes. Figure 6 shows the d_{norm} map and the associated 2D fingerprint plots. The extracted shape index and curvedness maps are illustrated in Figure 7.

As shown in Figure 6(i), the C···H/H···C contacts were noticed with obvious large red regions labeled 1 and exhibited 27.0% of the total HS area. Such contacts were also observed in the 2D fingerprint plots as a pair of symmetrical spikes at (d_e + d_i) ∼ 2.6 Å (Figure 6(ii)).

The existence of red regions dubbed 2 in the HSs mapped over the d_{norm} property could be attributed to the occurrence of the reciprocal O···H/H···O contacts that were found in the 2D fingerprint plots at (d_e + d_i) ∼ 2.3 Å. For S···H/H···S contacts (labeled 3), prominent red regions were noticed with 2.1% of the total HS area and characterized by spikes at (d_e + d_i) ∼ 2.7 Å. The N···H/H···N contacts were observed with label 4, as white and red regions in the d_{norm} maps, with a 2.1% contribution.

Table 2. Stoichiometric Formation and Analytical Data of Cu-Complexes 16a-f

ligand	metal salt	complex	stoichiometry	molecular formula	C, H, Cu, N, O, P, S,
15a	$CuCl_2{\cdot}2H_2O$	**16a**	1:1	$C_{49}H_{40}CuN_3O_3P_2S$	calcd: C, 67.15; H, 4.60; Cu, 7.25; N, 4.79; O, 5.48; P, 7.07; S, 3.66
					found: C, 67.17; H, 4.62; Cu, 7.23; N, 4.77; O, 5.50; P, 7.05; S, 3.64
15b	$CuCl_2{\cdot}2H_2O$	**16b**	1: 1	$C_{50}H_{40}CuN_3O_3P_2S$	calcd: C, 67.60; H, 4.54; Cu, 7.15; N, 4.73; O, 5.40; P, 6.97; S, 3.61
					found: C, 67.58; H, 4.56; Cu, 7.17; N, 4.71; O, 5.38; P, 6.95; S, 3.63
15c	$CuCl_2{\cdot}2H_2O$	**16c**	1:1	$C_{54}H_{42}CuN_3O_3P_2S$	calcd: C, 69.11; H, 4.51; Cu, 6.77; N, 4.48; O, 5.11; P, 6.60; S, 3.42
					found: C, 67.11; H, 4.53; Cu, 6.79; N, 4.50; O, 5.13; P, 6.58; S, 3.44
15d	$CuCl_2{\cdot}2H_2O$	**16d**	1:1	$C_{50}H_{42}CuN_3O_3P_2S$	calcd: C, 67.44; H, 4.75; Cu, 7.14; N, 4.72; O, 5.39; P, 6.96; S, 3.60
					found: C, 67.42; H, 4.77; Cu, 7.16; N, 4.70; O, 5.41; P, 6.98; S, 3.62
15e	$CuCl_2{\cdot}2H_2O$	**16e**	1:1	$C_{50}H_{40}CuN_3O_3P_2S$	calcd: C, 67.60; H, 4.54; Cu, 7.15; N, 4.73; O, 5.40; P, 6.97; S, 3.61
					found: C, 67.62; H, 4.52; Cu, 7.13; N, 4.75; O, 5.42; P, 6.99; S, 3.59
15f	$CuCl_2{\cdot}2H_2O$	**16f**	1:1	$C_{51}H_{44}CuN_3O_3P_2S$	calcd: C, 67.72; H, 4.90; Cu, 7.03; N, 4.65; O, 5.31; P, 6.85; S, 3.54
					found: C, 67.74; H, 4.92; Cu, 7.05; N, 4.63; O, 5.29; P, 6.85; S, 3.52

https://doi.org/10.1021/acsomega.2c04113
ACS Omega 2022, 7, 34463−34475

Table 3. IR Absorption Bands (υ, cm^{-1}) of Ligands 15a-f and Their Complexes of Cu(II) 16a-f

ligand	absorption of functional groups (ν) in ligands (cm^{-1})	metal complex	absorption of functional groups (ν) in complexes (cm^{-1})
15a	ν = 3345, 3052 (w, NH), 1587, 1517 (m, C=O), 1435 (s, C=N), 1188 (s, C=P), 993 cm^{-1} (s, C=S).	**16a**	ν = 3054 (w, NH), 1576, 1505 (m, C=O), 1482 (s, C=N), 1178 (s, C=P), 1019 (m, P=O), 995 (s, C=S), 536 (s, Cu−N), 457 cm^{-1} (s, Cu−O).
15b	ν = 3347, 3067 (w, NH), 1585, 1542 (m, C=O), 1431 (s, C=N), 1169 (vs, C=P), 990 cm^{-1} (vs, C=S).	**16b**	ν = 3055 (w, NH), 1572, 1503 (s, C=O), 1483 (s, C=N), 1187 (s, C=P), 1017 (vs, P=O), 1000 (vs, C=S), 557 (vs, Cu−N), 432 cm^{-1} (s, Cu−O).
15c	ν = 3340, 3055 (w, NH), 1582, 1510 (s, C=O), 1433 (s, C=N), 1153 (s, C=P), 988 cm^{-1} (vs, C=S).	**16c**	ν = 3077 (w, NH), 1577, 1514 (s, C=O), 1480 (s, C=N), 1157 (vs, C=P), 1017 (vs, P=O), 999 (s, C=S), 548 (vs, Cu−N), 453 cm^{-1} (vs, Cu−O).
15d	ν = 3347, 3052 (w, NH), 1580, 1507 (w, C=O), 1436 (s, C=N), 1188 (vs, C=P), 996 cm^{-1} (s, C=S).	**16d**	ν = 3051 (w, NH), 1589, 1513 (m, C=O), 1483 (s, C=N), 1163 (s, C=P), 1026 (w, P=O), 996 (m, C=S), 537 (vs, Cu−N), 449 cm^{-1} (s, Cu−O).
15e	ν = 3342, 3050 (w, NH), 1580, 1511(m, C=O), 1432 (s, C=N), 1186 (s, C=P), 996 cm^{-1} (s, C=S).	**16e**	ν = 3056 (w, NH), 1575, 1496 (m, C=O), 1483 (m, C=N), 1179 (vs, C=P), 1020 (s, P=O), 997 (s, C=S), 540 (vs, Cu−N), 460 cm^{-1} (s, Cu−O).
15f	ν = 3340, 3053 (w, NH), 1586, 1521 (m, C=O), 1434 (vs, C=N), 1170 (s, C=P), 992 cm^{-1} (s, C=S).	**16f**	ν = 3063 (w, NH), 1572, 1494 (m, C=O), 1466 (s, C=N), 1159 (vs, C=P), 1013 (vs, P=O), 1013 (vs, C=S), 547 (vs, Cu−N), 455 cm^{-1} (s, Cu−O).

Conspicuously, the HSs mapped over the shape index and curvedness properties (Figure 7) confirmed the occurrence of the C···H/H···C, O···H/H···O, S···H/H···S, and N···H/H···N interactions by the existence of the complementary pair of red and blue triangles in the shape index and the flat green area in curvedness.

3. EXPERIMENTAL SECTION

Uncorrected Melting points were taken in a Gallenkamp melting point apparatus (Weiss-Gallenkamp, Loughborough, UK). The infrared spectra were recorded with the Bruker, IFS 88 instrument. Solids were measured by the attenuated total reflection (ATR) method. The positions of the respective transmittance bands are given in wave numbers $\overline{\upsilon}$ [cm^{-1}] and were measured in the range from 3600 to 500 cm^{-1}. All UV−Vis spectra were recorded on the Specord 50 Plus made by the company Q Analytik Jena (Thuringia, Germany). The NMR spectra of the title compounds described herein were recorded on a Bruker Avance 400 NMR instrument at 400 MHz for ^{1}H NMR and 101 MHz for ^{13}C NMR, and the references used were the ^{1}H and ^{13}C peaks of the solvent, acetone-d_6: 2.05 ppm for ^{1}H NMR, and 206.26 ppm for ^{13}C{^{1}H}NMR spectra. For the characterization of centrosymmetric signals, the signal's median point was chosen; for multiplets, the signal range was given. The following abbreviations were used to describe the proton splitting pattern: d = doublet, t = triplet, m = multiplet, and dd = doublet of a doublet. The following abbreviations were used to distinguish between signals: H^{Ar} = aromatic-CH. Signals of the ^{13}C NMR spectra were assigned with the help of DEPT90 and DEPT135 and were specified in the following way: + = primary or tertiary carbon atoms (positive DEPT signal), − = secondary carbon atoms (negative DEPT signal), C_q = quaternary carbon atoms (no DEPT signal). Mass spectra were observed by FAB (Fast atom bombardment) experiments and were recorded using the Finnigan, MAT 90 (70 eV) instrument. Elemental analyses were performed on the Elementar Vario MICRO instrument. TLC silica plates coated with a fluorescence indicator from Merck (silica gel 60 F254, thickness 0.2 mm) were used to purify the crude products, and flash chromatography with Silica gel 60 (0.040 × 0.063 mm, Geduran) (Merck) was used. Solvents, including acetone-d_6, were purchased from Merck without further drying.

3.1. General Procedures. Compounds **14a-f** were prepared according to the literature.[23]

*3.1.1. General Procedure for the Synthesis of Ligands **15a-f**.* 2,3-Dichloro-1,4-naphthoquinone (7) (250 mg, 1.10 mmol, 1.10 equiv) was added to a stirred solution of substituted hydrazinecarbothioamides (**14a-f**) (1.00 mmol, 1.00 equiv) in 10 mL of dry CH_3CN. The resulting solution was stirred at room temperature for 16 h. After *S*-alkylation was complete (i.e. the reaction was followed up by TLC), the dried salt was redissolved in dry CH_3CN, after which Et_3N (1.10 mmol) and Ph_3P (1.10 mmol) were added. The resulting mixture was left under reflux for about 13−16 h. The reaction mixture was left to cool at room temperature, distilled H_2O (50 mL) was added, and the resulting solution was extracted with CH_2Cl_2. The organic extracts were dried over anhydrous $CaCl_2$, filtered, and evaporated. The crude material was purified by flash-chromatography using cyclohexane/ethyl acetate (4:1) to give compounds **15a-f**.

*3.1.1.1. (E)-2-(1,4-Dioxo-3-(triphenyl-λ^5-phosphaneylidene)-3,4-dihydronaphthalen-2(1H)-ylidene)-N-ethylhydrazine-1-carbothioamide (**15a**).* R_f = 0.27 (cyclohexane/ethyl acetate; 4:1). Violet crystals (MeOH), 0.385 g (72%). **mp**: 210−212 °C. **^{1}H NMR** (400 MHz, Acetone-d_6): δ_H = 12.90 (s, 1H, NH^1), 7.93 (dt, J = 44.4, 10.2 Hz, 2H, H^{Ar}), 7.84−7.68 (m, 2H, H^{Ar}), 7.65−7.31 (m, 15H, H^{Ar}), 5.77 (s, 1H, NH^2) 3.19−2.56 (m, 2H, CH_2^{ethyl}), 0.62 ppm (t, J = 7.1 Hz, 3H, CH_3^{ethyl}). **^{13}C{^{1}H}NMR** (101 MHz, Acetone-d_6): δ_C = 183.7 (C_q, *C*O), 183.6 (C_q, *C*O), 176.7 (C_q, *C*S), 142.8 (C_q, C=N), 137.2 (C_q, C^{Ar}), 137.1 (C_q, C^{Ar}), 134.5 (C_q, C^{Ar}), 134.1 (+, CH^{Ar}), 133.7 (+, CH^{Ar}), 133.6 (+, CH^{Ar}), 133.1 (+, CH^{Ar}), 132.8 (+, CH^{Ar}), 132.5 (+, CH^{Ar}), 132.4 (+, CH^{Ar}), 131.8 (+, 2× CH^{Ar}), 131.7 (+, 2× CH^{Ar}), 130.6 (+, CH^{Ar}), 129.1 (+, CH^{Ar}), 128.9 (+, CH^{Ar}), 128.6 (+, 2× CH^{Ar}), 128.5 (+, 2× CH^{Ar}), 126.6 (+, CH^{Ar}), 125.6 (C_q, C^{Ar}), 125.5 (C_q, C^{Ar}), 124.5 (C_q, C^{Ar}), 37.9 (−, CH_2^{ethyl}), 13.5 ppm (+, CH_3^{ethyl}). **IR** (ATR): $\tilde{\nu}$ = 3345, 3052 (w, NH), 1587, 1517 (m, C=O), 1435 (s, C=N), 1188 (s, C=P), 993 cm^{-1} (s, C=S). **MS** (FAB, 3-NBA): m/z (%) = 536 (100) [M + H]$^+$, 535 (30) [M]$^+$. **HRMS** (FAB, 3-NBA, $C_{31}H_{27}N_3O_2P_1{}^{32}S_1$, [M + H]$^+$) calcd: 536.1562; found: 536.1563. **EA** ($C_{31}H_{26}N_3O_2PS$) calcd: C, 69.52; H, 4.89; N, 7.85; O, 5.97; P, 5.78; S, 5.99. Found: C, 69.50; H, 4.87; N, 7.87; O, 5.99; P, 5.76; S, 5.97.

*3.1.1.2. (E)-N-Allyl-2-(1,4-dioxo-3-(triphenyl-λ^5-phosphaneylidene)-3,4-dihydronaphthalen-2(1H)-ylidene)hydrazine-1-carbothioamide (**15b**).* R_f = 0.29 (cyclohexane/ethyl acetate; 4:1). Violet crystals (MeOH), 0.415 g (76%). − **Mp**: 190−192 °C. **^{1}H NMR** (400 MHz, Acetone-d_6): δ_H = 12.96 (s, 1H, NH^1), 8.22−7.97 (m, 2H, H^{Ar}), 7.96−7.80 (m, 2H, H^{Ar}), 7.80−7.61 (m, 7H, H^{Ar}), 7.61−7.29 (m, 8H, H^{Ar}), 6.47 (s, 1H, NH^2), 5.82−5.71 (m, 1H, CH^{allyl}) 4.95−4.80 (m, 2H, CH_2^{allyl}), 4.22−3.61 ppm (m, 2H, CH_2^{allyl}). **^{13}C{^{1}H}NMR** (101 MHz, acetone-d_6): δ_C = 184.7 (C_q, *C*O), 184.6 (C_q, *C*O), 177.9 (C_q, *C*S), 142.1 (C_q, C=N), 138.1 (C_q, C^{Ar}), 135.4 (C_q,

https://doi.org/10.1021/acsomega.2c04113
ACS Omega 2022, 7, 34463−34475

Table 4. Chemical Shifts (δ), Including ^{1}H And/or ^{13}C NMR Spectroscopic Data for Ligand 15a and Its Complex 16a

ligand	^{1}H and ^{13}C NMR (δ,acetone-d_6)	metal complex	^{1}H and ^{13}C NMR (δ, acetone-d_6)
15a	δH = 12.90 (s, 1H, NH^1), 7.93 (dt, J = 44.4, 10.2 Hz, 2H, H^{Ar}), 7.84−7.68 (m, 2H, H^{Ar}), 7.65−7.31 (m, 15H, H^{Ar}), 5.77 (s, 1H, NH^2) 3.19−2.56 (m, 2H, CH_2^{ethyl}), 0.62 ppm (t, J = 7.1 Hz, 3H, CH_3^{ethyl}). δ_C = 183.7 (C_q, CO), 183.6 (C_q, CO), 176.7 (C_q, CS), 142.8 (C_q, C=N), 137.2 (C_q, C^{Ar}), 137.1 (C_q, C^{Ar}), 134.5 (C_q, C^{Ar}), 134.1 (+, CH^{Ar}), 133.7 (+, CH^{Ar}), 133.6 (+, CH^{Ar}), 133.1 (+, CH^{Ar}), 132.8 (+, CH^{Ar}), 132.5 (+, CH^{Ar}), 132.4 (+, CH^{Ar}), 131.8 (+, 2× CH^{Ar}) 131.7 (+, 2× CH^{Ar}), 130.6 (+, CH^{Ar}), 129.1 (+, CH^{Ar}), 128.9 (+, CH^{Ar}), 128.6 (+, 2× CH^{Ar}), 128.5 (+, 2× CH^{Ar}), 126.6 (+, CH^{Ar}), 125.6 (C_q, C^{Ar}), 125.5 (C_q, C^{Ar}), 124.5 (C_q, C^{Ar}), 37.9 (−, CH_2^{ethyl}), 13.5 ppm (+, CH_3^{ethyl}).	**16a**	δ_H = 7.73−7.65 (m, 15H, H^{Ar}), 7.64−7.58 (m, 6H, H^{Ar}), 7.56−7.50 (m, 13H, H^{Ar}), 5.49 (s, 1H, NH), 4.05 (q, J = 7.1 Hz, 2H, CH_2^{ethyl}), 1.20 ppm (t, J = 7.1 Hz, 3H, CH_3^{ethyl}). δ_C = 170.0 (C_q CO), 169.6 (C_q, CO), 165.4 (C_q, CS), 143.1 (C_q, C=N), 137.2 (C_q, C^{Ar}), 134.1 (+, 2× CH^{Ar}), 133.6 (C_q, C^{Ar}), 133.5 (C_q, C^{Ar}), 133.3 (+, 2× CH^{Ar}), 131.9 (+, 6× CH^{Ar}), 131.8 (+, 6× CH^{Ar}), 131.7 (+, 6× CH^{Ar}), 131.6 (+, 6× CH^{Ar}), 129.1 (+, 3× CH^{Ar}), 129.0 (+, 3× CH^{Ar}), 128.6 (C_q, 3× C^{Ar}), 128.5 (C_q, 3× C^{Ar}), 39.0 (−, CH_2^{ethyl}), 13.6 ppm (+, CH_3^{ethyl}).

C^{Ar}), 135.2 (C_q, C^{Ar}), 135.0 (+, CH^{Ar}), 134.7 (+, CH^{Ar}), 134.6 (+, CH^{Ar}), 134.5 (+, 2× CH^{Ar}), 134.5 (+, CH^{Ar}), 133.4 (+, CH^{Ar}), 133.3 (+, CH^{Ar}), 132.7 (+, CH^{Ar}), 132.6 (+, CH^{Ar}), 131.5 (+, CH^{allyl}), 130.4 (+, CH^{Ar}), 130.0 (+, 2× CH^{Ar}), 129.9 (+, CH^{Ar}), 129.8 (+, CH^{Ar}), 129.6 (+, CH^{Ar}), 129.5 (+, CH^{Ar}), 129.4 (+, CH^{Ar}), 127.5 (+, CH^{Ar}), 126.4 (C_q, C^{Ar}), 126.2 (C_q, C^{Ar}), 125.3 (C_q, C^{Ar}), 116.4 (−, CH_2^{allyl}), 46.3 ppm (−, CH_2^{allyl}).− **IR** (ATR): $\tilde{\nu}$ = 3347, 3067 (w, NH), 1585, 1542 (m, C═O), 1431 (s, C═N), 1169 (vs, C═P), 990 cm^{-1} (vs, C═S). **MS** (FAB, 3-NBA): m/z (%) = 548 (100) [M + H]$^+$, 547 (37) [M]$^+$. **HRMS** (FAB, 3-NBA, $C_{32}H_{27}N_3O_2P_1{}^{32}S_1$, [M + H]$^+$) calcd: 548.1556; found: 548.1557. **EA** ($C_{32}H_{26}N_3O_2PS$) calcd: C, 70.19; H, 4.79; N, 7.67; O, 5.84; P, 5.66; S, 5.85. Found: C, 70.21; H, 4.77; N, 7.69; O, 5.82; P, 5.68; S, 5.87.

*3.1.1.3. (E)-N-Benzyl-2-(1,4-dioxo-3-(triphenyl-λ^5-phosphaneylidene)-3,4-dihydronaphthalen-2(1H)-ylidene)-hydrazine-1-carbothioamide (**15c**).* R_f = 0.25 (cyclohexane/ethyl acetate; 4:1). Violet crystals (MeOH), 0.489 g (82%). **mp**: 220−222 °C. **^{1}H NMR** (400 MHz, acetone-d_6): δ_H = 13.04 (s, 1H, NH^1), 8.21−7.80 (m, 4H, H^{Ar}), 7.80−7.59 (m, 5H, H^{Ar}), 7.59−7.33 (m, 10H, H^{Ar}), 7.29−7.03 (m, 5H, H^{Ar}), 6.85 (s, 1H, NH^2), 4.38−4.20 ppm (m, 2H, CH_2^{benzyl}). **^{13}C{^{1}H}NMR** (101 MHz, acetone-d_6): δ_C = 177.2 (C_q, CO), 176.3 (C_q, CO), 162.8 (C_q, CS), 141.5 (C_q, C═N), 138.0 (C_q, C^{Ar}), 137.5 (C_q, C^{Ar}), 137.1 (C_q, C^{Ar}), 137.0 (C_q, C^{Ar}), 134.6 (+, CH^{Ar}), 133.7 (+, CH^{Ar}), 133.6 (+, 2× CH^{Ar}), 133.5 (+, 2× CH^{Ar}), 133.4 (+, CH^{Ar}), 132.4 (+, CH^{Ar}), 132.3 (+, CH^{Ar}), 130.6 (+, CH^{Ar}), 129.1 (+, 2× CH^{Ar}), 128.9 (+, 2× CH^{Ar}), 128.7 (+, CH^{Ar}), 128.6 (+, CH^{Ar}), 128.5 (+, CH^{Ar}), 128.3 (+, CH^{Ar}), 128.1 (+, CH^{Ar}), 127.9 (+, CH^{Ar}), 127.7 (+, CH^{Ar}), 127.2 (+, CH^{Ar}), 126.6 (+, CH^{Ar}), 125.5 (+, CH^{Ar}), 125.2 (C_q, C^{Ar}), 124.5 (C_q, C^{Ar}), 124.3 (C_q, C^{Ar}), 46.9 ppm (−, CH_2^{benzyl}).− **IR** (ATR): $\tilde{\nu}$ = 3340, 3055 (w, NH), 1582, 1510 (s, C═O), 1433 (s, C═N), 1153 (s, C═P), 988 cm^{-1} (vs, C═S). **MS** (FAB, 3-NBA): m/z (%) = 598 (75) [M + H]$^+$, 597 (30) [M]$^+$. **HRMS** (FAB, 3-NBA, $C_{36}H_{29}N_3O_2P_1{}^{32}S_1$, [M + H]$^+$) calcd: 598.1718; found: 598.1717. **EA** ($C_{36}H_{28}N_3O_2PS$) calcd: C, 72.35; H, 4.72; N, 7.03; O, 5.35; P, 5.18; S, 5.36. Found: C, 72.37; H, 4.74; N, 7.01; O, 5.33; P, 5.16; S, 5.38.

*3.1.1.4. (E)-2-(1,4-Dioxo-3-(triphenyl-λ^5-phosphaneylidene)-3,4-dihydronaphthalen-2(1H)-ylidene)-N-isopropylhydrazine-1-carbothioamide (**15d**).* R_f = 0.26 (cyclohexane/ethyl acetate; 4:1). Violet crystals (MeOH), 0.406 g (74%). **mp**: 200−202 °C. **^{1}H NMR** (400 MHz, acetone-d_6): δ_H = 12.82 (s, 1H, NH^1), 8.28−7.87 (m, 4H, H^{Ar}), 7.87−7.59 (m, 5H, H^{Ar}), 7.59−7.16 (m, 10H, H^{Ar}), 5.83 (s, 1H, NH^2), 4.12−3.75 (m, 1H, $CH^{Isopropyl}$), 1.50−1.03 ppm (m, 6H, 2× $CH_3^{Isopropyl}$). **^{13}C{^{1}H}NMR** (101 MHz, acetone-d_6): δ_C = 184.5 (C_q, CO), 184.4 (C_q, CO), 178.2 (C_q, CS), 147.3 (C_q, C═N), 138.3 (C_q, C^{Ar}), 135.1 (C_q, C^{Ar}), 134.8 (C_q, C^{Ar}), 134.7 (+, CH^{Ar}), 134.0 (+, CH^{Ar}), 133.5 (+,CH^{Ar}), 133.4 (+,CH^{Ar}), 132.9 (+, 2× CH^{Ar}), 132.8 (+, CH^{Ar}), 132.7 (+, CH^{Ar}), 132.6 (+, 2× CH^{Ar}), 131.5 (+, CH^{Ar}), 130.1 (+, CH^{Ar}), 129.9 (+, CH^{Ar}), 129.5 (+, 2× CH^{Ar}), 129.4 (+, 2× CH^{Ar}), 127.5 (+, CH^{Ar}), 127.3 (+, CH^{Ar}), 126.6 (C_q, C^{Ar}), 126.1 (C_q, C^{Ar}), 125.2 (C_q, C^{Ar}), 45.9 (+, $CH^{Isopropyl}$), 22.2 ppm (+, 2× $CH_3^{Isopropyl}$). **IR** (ATR): $\tilde{\nu}$ = 3347, 3052 (w, NH), 1580, 1507 (w, C═O), 1436 (s, C═N), 1188 (vs, C═P), 996 cm^{-1} (s, C═S). **MS** (FAB, 3-NBA): m/z (%) = 550 (100) [M + H]$^+$, 549 (28) [M]$^+$. **HRMS** (FAB, 3-NBA $C_{32}H_{29}N_3O_2P_1{}^{32}S_1$, [M + H]$^+$) calcd: 550.1718; found: 550.1719. **EA**

https://doi.org/10.1021/acsomega.2c04113
ACS Omega 2022, 7, 34463−34475

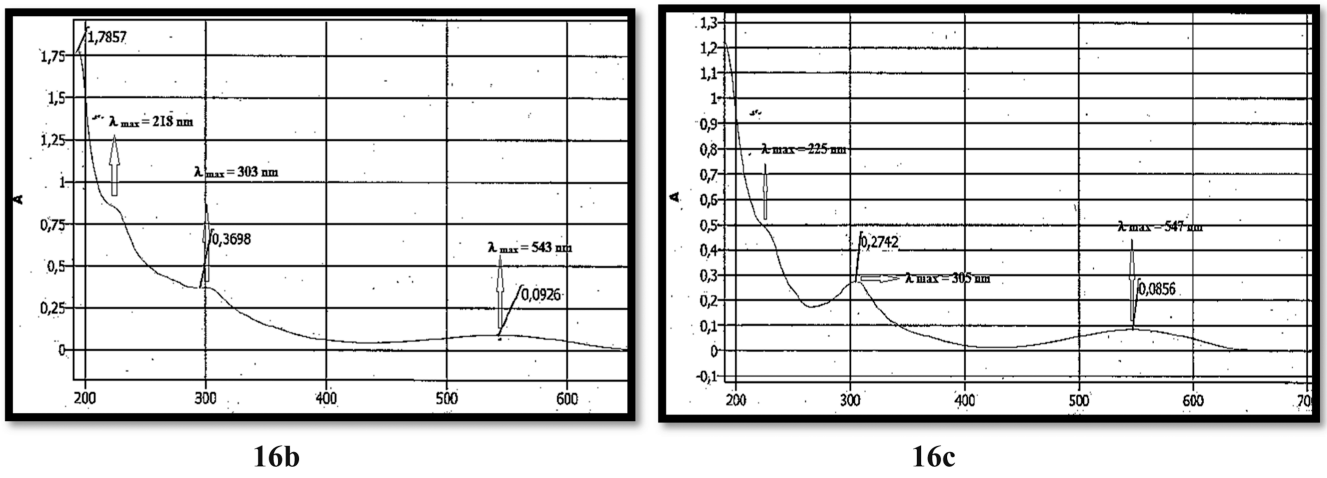

Figure 4. UV spectra of **16b** and **16c** in CH_3CN.

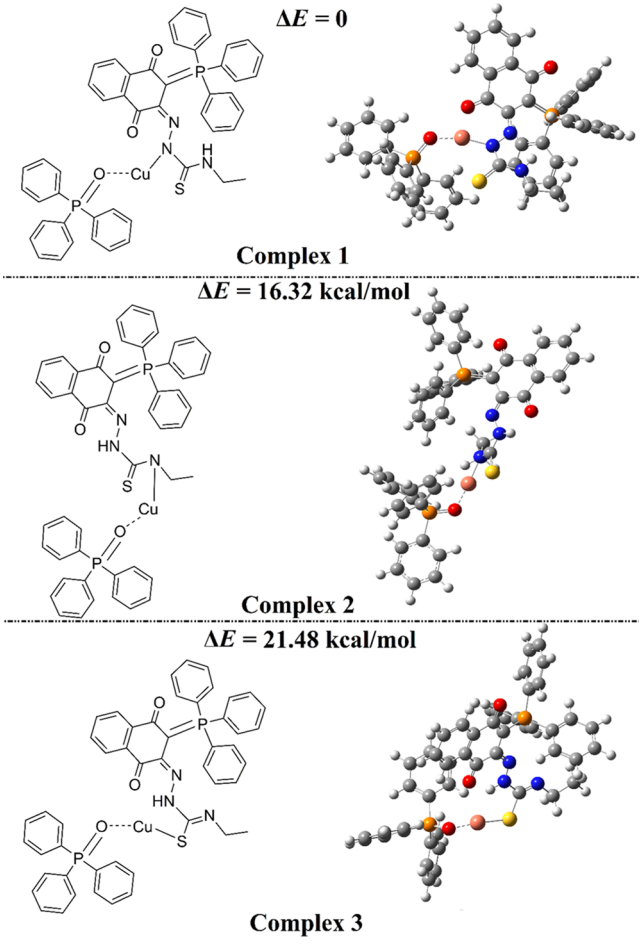

Figure 5. Optimized geometries of the studied complexes along with the energy difference (ΔE) between the investigated complex (E) and the most stable one (E_1).

($C_{32}H_{28}N_3O_2PS$) calcd: C, 69.93; H, 5.14; N, 7.65; O, 5.82; P, 5.64; S, 5.83. Found: C, 69.95; H, 5.16; N, 7.63; O, 5.80; P, 5.62; S, 5.81.

*3.1.1.5. (E)-N-Cyclopropyl-2-(1,4-dioxo-3-(triphenyl-λ^5-phosphaneylidene)-3,4-dihydronaphthalen-2(1H)-ylidene)-hydrazine-1-carbothioamide (**15e**).* R_f = 0.24 (cyclohexane/ethyl acetate; 4:1). Violet crystals (MeOH), 0.426 g (78%). **mp**: 205−207 °C. **^{1}H NMR** (400 MHz, acetone-d_6): δ_H = 13.09 (s, 1H, NH^1), 8.41−8.14 (m, 4H, H^{Ar}), 8.11−7.80 (m, 3H, H^{Ar}), 7.80−7.43 (m, 12H, H^{Ar}), 5.99 (s, 1H, NH^2), 2.83−2.55 (m, 1H, C$H^{Cyclopropyl}$), 0.71−0.51 ppm (m, 4H, 2× C$H_2^{Cyclopropyl}$). **^{13}C{^{1}H}NMR** (101 MHz, acetone-d_6): δ_C = 183.6 (C_q, CO), 183.5 (C_q, CO), 178.2 (C_q, CS), 141.9 (C_q, C═N), 137.2 (C_q, C^{Ar}), 137.1 (C_q, C^{Ar}), 134.6 (C_q, C^{Ar}), 134.3 (+, CH^{Ar}), 134.2 (+, CH^{Ar}), 133.7 (+, CH^{Ar}), 133.6 (+, CH^{Ar}), 132.7 (+, CH^{Ar}), 132.5 (+, CH^{Ar}), 132.0 (+,CH^{Ar}), 131.9 (+, 2× CH^{Ar}), 131.8 (+, CH^{Ar}), 131.7 (+, CH^{Ar}), 130.6 (+, CH^{Ar}), 129.1 (+, CH^{Ar}), 129.0 (+, CH^{Ar}), 128.9 (+, CH^{Ar}), 128.8 (+, CH^{Ar}), 128.6 (+, CH^{Ar}), 128.5 (+, 2× CH^{Ar}), 126.5 (C_q, C^{Ar}), 125.1 (C_q, C^{Ar}), 124.2 (C_q, C^{Ar}), 25.8 (+, $CH^{Cyclopropyl}$), 6.5 ppm (−, 2× $CH_2^{Cyclopropyl}$). **IR** (ATR): $\tilde{\nu}$ = 3342, 3050 (w, NH), 1580, 1511 (m, C═O), 1432 (s, C═N), 1186 (s, C═P), 996 cm^{-1} (s, C═S). **MS** (FAB, 3-NBA): m/z (%) = 548 (100) $[M + H]^+$, 547 (35) $[M]^+$. **HRMS** (FAB, 3-NBA, $C_{32}H_{27}N_3O_2P_1{}^{32}S_1$, $[M + H]^+$) calcd: 548.1562; found: 548.1563. **EA** ($C_{32}H_{26}N_3O_2PS$) calcd: C, 70.19; H, 4.79; N, 7.67; O, 5.84; P, 5.66; S, 5.85. Found: C, 70.17; H, 4.81; N, 7.69; O, 5.82; P, 5.64; S, 5.83.

*3.1.1.6. (E)-N-Butyl-2-(1,4-dioxo-3-(triphenyl-λ^5-phosphaneylidene)-3,4-dihydronaphthalen-2(1H)-ylidene)hydrazine-1-carbothioamide (**15f**).* R_f = 0.28 (cyclohexane/ethyl acetate; 4:1). Violet crystals (MeOH), 0.450 g (80%). **mp**: 195−197 °C. **^{1}H NMR** (400 MHz, acetone-d_6): δ_H = 13.18 (s, 1H, NH^1), 8.10−8.00 (m, 2H, H^{Ar}), 7.66−7.55 (m, 8H, H^{Ar}), 7.28−7.24 (m, 9H, H^{Ar}), 6.74 (s, 1H, NH^2), 3.58 (dd, J = 7.7, 1.5 Hz, 2H, CH_2^{butyl}) 1.60−1.49 (m, 2H, CH_2^{butyl}), 1.35−1.26 (m, 2H, CH_2^{butyl}), 1.02−0.99 ppm (m, 3H, CH_3^{butyl}). **^{13}C-{^{1}H}NMR** (101 MHz, acetone-d_6): δ_C = 186.1 (C_q, CO), 185.9 (C_q, CO), 178.4 (C_q, CS), 142.3 (C_q, C═N), 135.1 (C_q, C^{Ar}), 134.6 (C_q, C^{Ar}), 134.1 (C_q, C^{Ar}), 132.7 (+, CH^{Ar}), 132.6 (+, CH^{Ar}), 132.3 (+, CH^{Ar}), 131.7 (+, 3× CH^{Ar}), 131.3 (+, CH^{Ar}), 131.1 (+, CH^{Ar}), 130.7 (+, 3× CH^{Ar}), 130.5 (+, CH^{Ar}), 130.4 (+, CH^{Ar}), 129.9 (+, CH^{Ar}), 129.5 (+, CH^{Ar}), 129.4 (+, CH^{Ar}), 129.3 (+, CH^{Ar}), 128.7 (+, 2× CH^{Ar}), 128.1 (C_q, C^{Ar}), 127.8 (C_q, C^{Ar}), 127.7 (C_q, C^{Ar}), 44.6 (−, CH_2^{butyl}), 30.4 (−, CH_2^{butyl}), 20.1 (−, CH_2^{butyl}), 14.0 ppm (+, CH_3^{butyl}). **IR** (ATR): $\tilde{\nu}$ = 3340, 3053 (w, NH), 1586, 1521 (m, C═O), 1434 (vs, C═N), 1170 (s, C═P), 992 cm^{-1} (s, C═S). **MS** (FAB, 3-NBA): m/z (%) = 564 (100) $[M + H]^+$, 563 (30) $[M]^+$. **HRMS** (FAB, 3-NBA, $C_{33}H_{31}N_3O_2P_1{}^{32}S_1$, $[M + H]^+$) calcd: 564.1875; found: 564.1873. **EA** ($C_{33}H_{30}N_3O_2PS$) calcd:

https://doi.org/10.1021/acsomega.2c04113
ACS Omega 2022, 7, 34463−34475

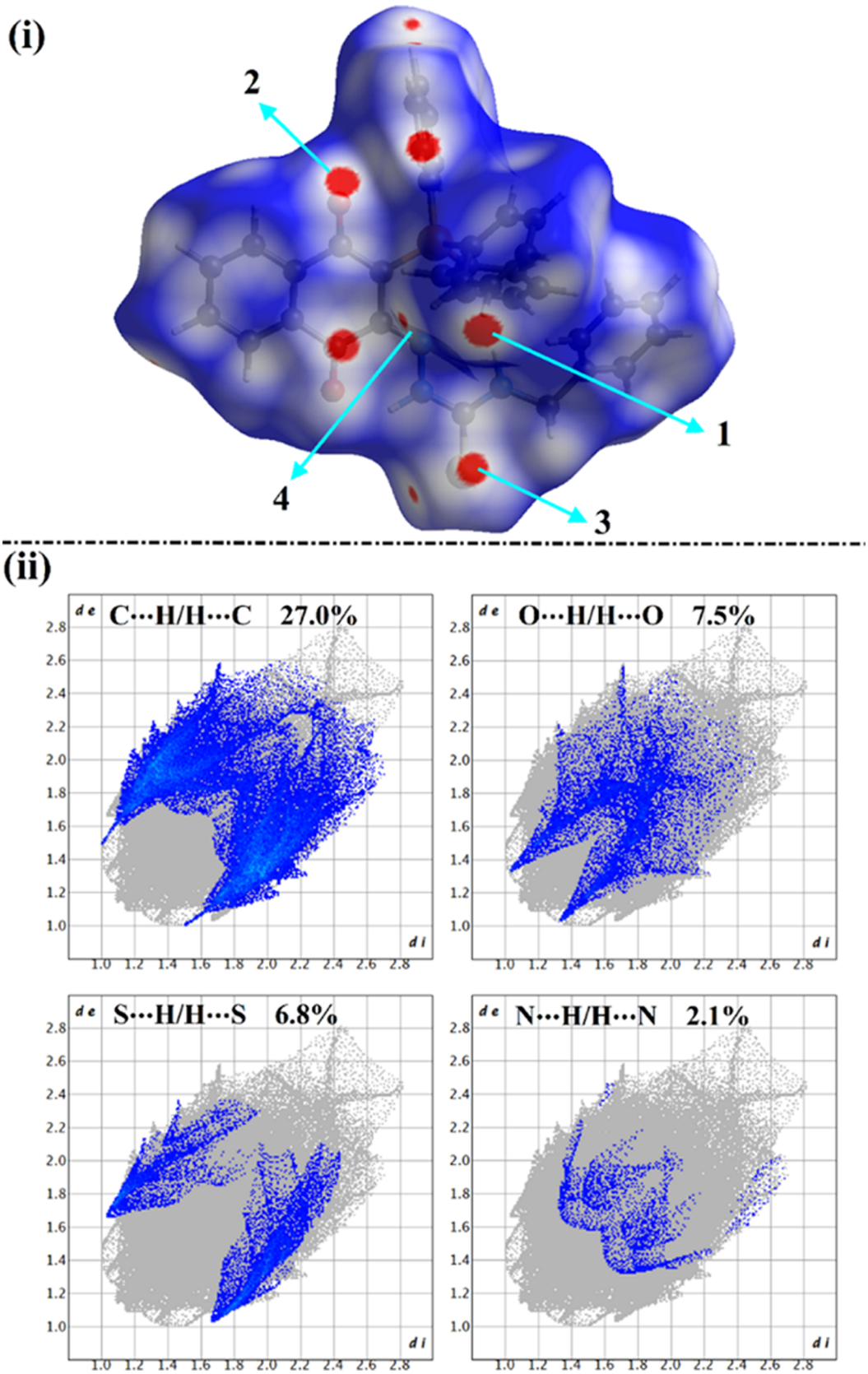

Figure 6. Views of (i) HSs mapped over the d_{norm} property; the labels 1, 2, 3, and 4 represent C···H/H···C, O···H/H···O, S···H/H···S, and N···H/H···N contacts, respectively; and (ii) 2D fingerprint plots for the interactions above.

C, 70.32; H, 5.36; N, 7.46; O, 5.68; P, 5.50; S, 5.69. Found: C, 70.34; H, 5.38; N, 7.44; O, 5.66; P, 5.52; S, 5.67.

*3.1.2. General Procedure for the Synthesis of Complexes **16a-f.*** A mixture of **15a-f** (1.00 mmol, 1.00 equiv) with $CuCl_2$·

https://doi.org/10.1021/acsomega.2c04113
ACS Omega 2022, 7, 34463−34475

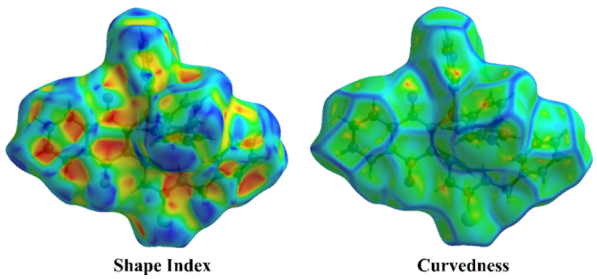

Figure 7. HSs mapped over the shape index and curvedness properties.

$2H_2O$ (0.170 g, 1.00 mmol, 1.00 equiv) and Ph_3P (0.262 g, 1.00 mmol, 1.00 equiv) in 40 mL of absolute EtOH was stirred at room temperature for about 2−4 h (the reaction was monitored by thin-layer chromatography). After removal of the solvent under reduced pressure, the crude product was purified by column chromatography using EtOAc/hexane (5:1) to afford compounds **16a**−**f**.

*3.1.2.1. (E)-(2-(1,4-Dioxo-3-(triphenyl-λ⁵-phosphaneylidene)-3,4-dihydronaphthalen-2(1H)-ylidene)-1-(ethylcarbamothioyl)hydrazineyl) ((triphenyl-λ⁵-phosphaneyl)oxy)copper (**16a**).* R_f = 0.35 (cyclohexane/ethyl acetate; 4:1). Deep blue crystals (MeOH), 0.718 g (82%). **mp**: 250−252 °C (decomp). **^{1}H NMR** (400 MHz, acetone-d_6): δ_H = 7.73−7.65 (m, 15H, H^{Ar}), 7.64−7.58 (m, 6H, H^{Ar}), 7.56−7.50 (m, 13H, H^{Ar}), 5.49 (s, 1H, N*H*), 4.05 (q, J = 7.1 Hz, 2H, CH_2^{ethyl}), 1.20 ppm (t, J = 7.1 Hz, 3H, CH_3^{ethyl}). **^{13}C{^{1}H}NMR** (101 MHz, acetone-d_6): δ_C = 170.0 (C_q, CO), 169.6 (C_q, CO), 165.4 (C_q, CS), 143.1 (C_q, C=N), 137.2 (C_q, C^{Ar}), 134.1 (+, 2× CH^{Ar}), 133.6 (C_q, C^{Ar}), 133.5 (C_q, C^{Ar}), 133.3 (+, 2× CH^{Ar}), 131.9 (+, 6× CH^{Ar}), 131.8 (+, 6× CH^{Ar}), 131.7 (+, 6× CH^{Ar}), 131.6 (+, 6× CH^{Ar}), 129.1 (+, 3× CH^{Ar}), 129.0 (+, 3× CH^{Ar}), 128.6 (C_q, 3× C^{Ar}), 128.5 (C_q, 3× C^{Ar}), 39.0 (−, CH_2^{ethyl}), 13.6 ppm (+, CH_3^{ethyl}). **IR** (ATR): $\tilde{\nu}$ = 3054 (w, NH), 1576, 1505 (m, C=O), 1482 (s, C=N), 1178 (s, C=P), 1019 (m, P=O), 995 (s, C=S), 536 (s, Cu−N), 457 cm^{-1} (s, Cu−O). **MS** (FAB, 3-NBA): m/z (%) = 875 (65) $[M]^+$. **HRMS** (FAB, 3-NBA, $C_{49}H_{40}CuN_3O_3P_2{}^{32}S_1$, $[M]^+$) calcd: 875.1562; found: 875.1563. **EA** ($C_{49}H_{40}CuN_3O_3P_2S$) calcd: C, 67.15; H, 4.60; Cu, 7.25; N, 4.79; O, 5.48; P, 7.07; S, 3.66. Found: C, 67.17; H, 4.62; Cu, 7.23; N, 4.77; O, 5.50; P, 7.05; S, 3.64.

*3.1.2.2. (E)-(1-(Allylcarbamothioyl)-2-(1,4-dioxo-3-(triphenyl-λ⁵-phosphaneylidene)-3,4-dihydronaphthalen-2(1H)-ylidene)hydrazineyl) ((triphenyl-λ⁵-phosphaneyl)oxy)copper (**16b**).* R_f = 0.33 (cyclohexane/ethyl acetate; 4:1). Deep blue crystals (MeOH), 0.745 g (84%). **mp**: 244−246 °C (decomp). **^{1}H NMR** (400 MHz, acetone-d_6): δ_H = 7.83−7.70 (m, 12H, H^{Ar}), 7.67−7.57 (m, 4H, H^{Ar}), 7.56−7.49 (m, 12H, H^{Ar}), 7.45−7.27 (m, 6H, H^{Ar}), 6.02−5.87 (m, 1H, CH^{allyl}), 5.65 (s, 1H, N*H*), 5.35−5.02 (m, 2H, CH_2^{allyl}), 4.42−3.91 ppm (m, 2H, CH_2^{allyl}). **^{13}C{^{1}H}NMR** (101 MHz, Acetone-d_6): δ_C = 172.7 (C_q, CO), 172.6 (C_q, CO), 167.9 (C_q, CS), 144.4 (C_q, C=N), 138.6 (C_q, C^{Ar}), 134.6 (+, 2× CH^{Ar}), 134.5 (C_q, C^{Ar}), 134.3 (C_q, C^{Ar}), 133.8 (+, 2× CH^{Ar}), 133.3 (+, 4× CH^{Ar}), 132.7 (+, 4× CH^{Ar}), 132.4 (+, 4× CH^{Ar}), 131.5 (+, 4× CH^{Ar}), 130.5 (+, CH^{allyl}), 129.9 (+, 3× CH^{Ar}), 129.7 (+, 3× CH^{Ar}), 129.5 (+, 2× CH^{Ar}), 129.4 (+, 2× CH^{Ar}), 128.3 (+, 2× CH^{Ar}), 127.4 (+, 2× CH^{Ar}), 126.5 (C_q, 3× C^{Ar}), 125.2 (C_q, 3× C^{Ar}), 116.3 (−, CH_2^{allyl}), 46.6 ppm (−, CH_2^{allyl}). **IR** (ATR): $\tilde{\nu}$ = 3055 (w, NH), 1572, 1503 (s, C=O), 1483 (s, C=N), 1187 (s, C=P), 1017 (vs, P=O), 1000 (vs, C=S), 557 (vs, Cu−N), 432 cm^{-1} (s, Cu−O). **MS** (FAB, 3-NBA): m/z (%) = 887 (60) $[M]^+$. **HRMS** (FAB, 3-NBA, $C_{50}H_{40}CuN_3O_3P_2{}^{32}S_1$, $[M]^+$) calcd: 887.1562; found: 887.1563. **EA** ($C_{50}H_{40}CuN_3O_3P_2S$) calcd: C, 67.60; H, 4.54; Cu, 7.15; N, 4.73; O, 5.40; P, 6.97; S, 3.61. Found: C, 67.58; H, 4.56; Cu, 7.17; N, 4.71; O, 5.38; P, 6.95; S, 3.63.

*3.1.2.3. (E)-(1-(Benzylcarbamothioyl)-2-(1,4-dioxo-3-(triphenyl-λ⁵-phosphaneylidene)-3,4-dihydronaphthalen-2(1H)-ylidene)hydrazineyl) ((triphenyl-λ⁵-phosphaneyl)oxy)copper (**16c**).* R_f = 0.36 (cyclohexane/ethyl acetate; 4:1). Deep blue crystals (MeOH), 0.872 g (93%). **mp**: 262−264 °C (decomp). **^{1}H NMR** (400 MHz, acetone-d_6): δ_H = 8.25−7.75 (m, 4H, H^{Ar}), 7.74−7.62 (m, 15H, H^{Ar}), 7.61−7.39 (m, 15H, H^{Ar}), 7.38−7.07 (m, 5H, H^{Ar}), 5.36 (s, 1H, N*H*), 4.36−4.23 ppm (m, 2H, CH_2^{benzyl}). **^{13}C{^{1}H}NMR** (101 MHz, acetone-d_6): δ_C = 172.6 (C_q, CO), 172.4 (C_q, CO), 170.9 (C_q, CS), 143.5 (C_q, C=N), 137.1 (C_q, C^{Ar}), 134.9 (C_q, C^{Ar}), 134.4 (C_q, C^{Ar}), 133.9 (C_q, C^{Ar}), 133.3 (+, CH^{Ar}), 132.6 (+, CH^{Ar}), 132.5 (+, CH^{Ar}), 132.1 (+, 4× CH^{Ar}), 131.9 (+, 4× CH^{Ar}), 131.2 (+, CH^{Ar}), 130.7 (+, CH^{Ar}), 130.4 (+, CH^{Ar}), 129.8 (+, 3× CH^{Ar}), 129.7 (+, 4× CH^{Ar}), 129.4 (+, 4× CH^{Ar}), 128.9 (+, CH^{Ar}), 128.3 (+, 2× CH^{Ar}), 128.2 (+, 2× CH^{Ar}), 127.7 (+, 2× CH^{Ar}), 127.1 (+, 2× CH^{Ar}), 126.8 (+, CH^{Ar}), 126.4 (+, CH^{Ar}), 126.1 (+, CH^{Ar}), 125.9 (+, CH^{Ar}), 125.8 (+, CH^{Ar}), 125.3 (C_q, 3× C^{Ar}), 125.2 (C_q, 3× C^{Ar}), 46.3 ppm (−, CH_2^{benzyl}). **IR** (ATR): $\tilde{\nu}$ = 3077 (w, NH), 1577, 1514 (s, C=O), 1480 (s, C=N), 1157 (vs, C=P), 1017 (vs, P=O), 999 (s, C=S), 548 (vs, Cu−N), 453 cm^{-1} (vs, Cu−O). **MS** (FAB, 3-NBA): m/z (%) = 937 (75) $[M]^+$. **HRMS** (FAB, 3-NBA, $C_{54}H_{42}CuN_3O_3P_2{}^{32}S_1$, $[M]^+$) calcd: 937.1718; found: 937.1719. **EA** ($C_{54}H_{42}CuN_3O_3P_2S$) calcd: C, 69.11; H, 4.51; Cu, 6.77; N, 4.48; O, 5.11; P, 6.60; S, 3.42. Found: C, 67.11; H, 4.53; Cu, 6.79; N, 4.50; O, 5.13; P, 6.58; S, 3.44.

*3.1.2.4. (E)-(2-(1,4-Dioxo-3-(triphenyl-λ⁵-phosphaneylidene)-3,4-dihydronaphthalen-2(1H)-ylidene)-1-(isopropylcarbamothioyl)hydrazineyl) ((triphenyl-λ⁵-phosphaneyl)oxy)copper (**16d**).* R_f = 0.31 (cyclohexane/ethyl acetate; 4:1). Deep blue crystals (MeOH), 0.712 g (80%). **mp**: 268−270 °C. **^{1}H NMR** (400 MHz, acetone-d_6): δ_H = 7.78−7.68 (m, 13H, H^{Ar}), 7.63−7.57 (m, 6H, H^{Ar}), 7.56−7.47 (m, 15H, H^{Ar}), 5.63 (s, 1H, N*H*), 4.14−3.85 (m, 1H, $CH^{Isopropyl}$), 1.45−1.23 ppm (m, 6H, 2× $CH_3^{Isopropyl}$). **^{13}C{^{1}H}NMR** (101 MHz, acetone-d_6): δ_C = 173.1 (C_q, CO), 172.9 (C_q, CO), 170.1 (C_q, CS), 144.4 (C_q, C=N), 135.2 (C_q, C^{Ar}), 134.1 (C_q, C^{Ar}), 133.7 (C_q, C^{Ar}), 133.4 (+, CH^{Ar}), 132.8 (+, 5× CH^{Ar}), 132.7 (+, 5× CH^{Ar}), 132.6 (+, 5× CH^{Ar}), 132.5 (+, 5× CH^{Ar}), 132.4 (+, CH^{Ar}), 130.4 (+, CH^{Ar}), 129.8 (+, CH^{Ar}), 129.5 (+, 5× CH^{Ar}), 129.3 (+, 5× CH^{Ar}), 127.0 (C_q, 3× C^{Ar}), 126.7 (C_q, 3× C^{Ar}), 46.4 (+, $CH^{Isopropyl}$), 22.7 ppm (+, 2× $CH_3^{Isopropyl}$). **IR** (ATR): $\tilde{\nu}$ = 3051 (w, NH), 1589, 1513 (m, C=O), 1483 (s, C=N), 1163 (s, C=P), 1026 (w, P=O), 996 (m, C=S), 537 (vs, Cu−N), 449 cm^{-1} (s, Cu−O). **MS** (FAB, 3-NBA): m/z (%) = 889 (55) $[M]^+$. **HRMS** (FAB, 3-NBA, $C_{54}H_{42}CuN_3O_3P_2{}^{32}S_1$, $[M]^+$) calcd: 889.1713; found: 889.1716. − **EA** ($C_{50}H_{42}CuN_3O_3P_2S$) calcd: C, 67.44; H, 4.75; Cu, 7.14; N, 4.72; O, 5.39; P, 6.96; S, 3.60. Found: C, 67.42; H, 4.77; Cu, 7.16; N, 4.70; O, 5.41; P, 6.98; S, 3.62.

*3.1.2.5. (E)-(1-(Cyclopropylcarbamothioyl)-2-(1,4-dioxo-3-(triphenyl-λ⁵-phosphaneylidene)-3,4-dihydronaphthalen-2(1H)-ylidene)hydrazineyl) ((triphenyl-λ⁵-phosphaneyl)oxy)copper (**16e**).* R_f = 0.32 (cyclohexane/ethyl acetate; 4:1). Deep blue crystals (MeOH), 0.763 g (86%). **mp**: 249−251 °C

https://doi.org/10.1021/acsomega.2c04113
ACS Omega 2022, 7, 34463−34475

(decomp). **^{1}H NMR** (400 MHz, acetone-d_6): δ_H = 8.16−7.84 (m, 13H, H^{Ar}), 7.77−7.65 (m, 6H, H^{Ar}), 7.63−7.41 (m, 15H, H^{Ar}), 5.62 (s, 1H, N*H*), 1.44−1.17 (m, 1H, C$H^{Cyclopropyl}$), 0.95−0.79 ppm (m, 4H, 2× C$H_2^{Cyclopropyl}$). **^{13}C{^{1}H}NMR** (101 MHz, acetone-d_6): δ_C = 176.4 (C_q, CO), 176.1 (C_q, CO), 169.8 (C_q, CS), 144.1 (C_q, C═N), 135.2 (C_q, C^{Ar}), 135.1 (C_q, C^{Ar}), 135.0 (C_q, C^{Ar}), 134.8 (+, CH^{Ar}), 134.7 (+, 3× CH^{Ar}), 134.6 (+, 3× CH^{Ar}), 134.2 (+, 3× CH^{Ar}), 134.1 (+, 3× CH^{Ar}), 134.0 (+, CH^{Ar}), 133.5 (+, CH^{Ar}), 133.4 (+, CH^{Ar}), 132.9 (+, 4× CH^{Ar}), 132.8 (+, 4× CH^{Ar}), 132.7 (+, CH^{Ar}), 132.6 (+, CH^{Ar}), 132.5 (+, CH^{Ar}), 130.5 (+, CH^{Ar}), 130.3 (+, CH^{Ar}), 129.8 (+, CH^{Ar}), 129.6 (+, CH^{Ar}), 129.5 (+, CH^{Ar}), 129.4 (+, CH^{Ar}), 127.2 (+, CH^{Ar}), 125.5 (C_q, 3× C^{Ar}), 124.6 (C_q, 3× C^{Ar}), 23.3 (+, C$H^{Cyclopropyl}$), 8.9 ppm (−, 2× $CH_2^{Cyclopropyl}$). **IR** (ATR): $\tilde{\nu}$ = 3056 (w, NH), 1575, 1496 (m, C═O), 1483 (m, C═N), 1179 (vs, C═P), 1020 (s, P═O), 997 (s, C═S), 540 (vs, Cu−N), 460 cm^{-1} (s, Cu−O). **MS** (FAB, 3-NBA): *m*/*z* (%) = 887 (70) [M]$^+$. **HRMS** (FAB, 3-NBA, $C_{50}H_{40}CuN_3O_3P_2{}^{32}S_1$, [M]$^+$) calcd: 887.1562; found: 887.1563. **EA** ($C_{50}H_{40}CuN_3O_3P_2S$) calcd: C, 67.60; H, 4.54; Cu, 7.15; N, 4.73; O, 5.40; P, 6.97; S, 3.61. Found: C, 67.62; H, 4.52; Cu, 7.13; N, 4.75; O, 5.42; P, 6.99; S, 3.59.

*3.1.2.6. (E)-(1-(Butylcarbamothioyl)-2-(1,4-dioxo-3-(triphenyl-λ^5-phosphaneylidene)-3,4-dihydronaphthalen-2(1H)-ylidene)hydrazineyl) ((triphenyl-λ^5-phosphaneyl)oxy)-copper (**16f**).* R_f = 0.34 (cyclohexane/ethyl acetate; 4:1). Deep blue crystals (MeOH), 0.795 g (88%). **mp**: 257−259 °C (decomp). **^{1}H NMR** (400 MHz, acetone-d_6): δ_H = δ 8.33−7.99 (m, 13H, H^{Ar}), 7.89−7.79 (m, 6H, H^{Ar}), 7.75−7.54 (m, 15H, H^{Ar}), 5.35 (s, 1H, N*H*), 3.83−3.74 (m, 2H, CH_2^{butyl}) 1.47−1.23 (m, 4H 2× CH_2^{Butyl}), 0.93−0.76 ppm (m, 3H, CH_3^{Butyl}). **^{13}C{^{1}H}NMR** (101 MHz, acetone-d_6): δ_C = 173.72 (C_q, CO), 173.58 (C_q, CO), 171.08 (C_q, CS), 143.61 (C_q, C═N), 136.17 (C_q, C^{Ar}), 135.96 (C_q, C^{Ar}), 135.71 (C_q, C^{Ar}), 135.50 (+, CH^{Ar}), 135.36 (+, CH^{Ar}), 135.34 (+, 3× CH^{Ar}), 135.16 (+, 3× CH^{Ar}), 135.12 (+, 4× CH^{Ar}), 135.03 (+, CH^{Ar}), 134.43 (+, CH^{Ar}), 134.01 (+, CH^{Ar}), 133.50 (+, 4× CH^{Ar}), 133.02 (+, 4× CH^{Ar}), 132.64 (+, CH^{Ar}), 132.50 (+, CH^{Ar}), 132.31 (+, CH^{Ar}), 132.12 (+, CH^{Ar}), 131.67 (+, CH^{Ar}), 131.37 (+, CH^{Ar}), 131.16 (+, CH^{Ar}), 130.82 (+, CH^{Ar}), 130.48 (+, CH^{Ar}), 130.27 (+, CH^{Ar}), 129.83 (+, CH^{Ar}), 129.35 (C_q, 3× C^{Ar}), 128.81 (C_q, 3× C^{Ar}), 44.9 (−, CH_2^{Butyl}), 30.9 (−, CH_2^{Butyl}), 20.5 (−, CH_2^{Butyl}), 14.4 ppm (+, CH_3^{Butyl}). **IR** (ATR): $\tilde{\nu}$ = 3063 (w, NH), 1572, 1494 (m, C═O), 1466 (s, C═N), 1159 (vs, C═P), 1013 (vs, P═O), 1013 (vs, C═S), 547 (vs, Cu−N), 455 cm^{-1} (s, Cu−O). **MS** (FAB, 3-NBA): *m*/*z* (%) = 903 (50) [M]$^+$. **HRMS** (FAB, 3-NBA, $C_{51}H_{44}CuN_3O_3P_2{}^{32}S_1$, [M]$^+$) calcd: 903.1875; found: 903.1876. **EA** ($C_{51}H_{44}CuN_3O_3P_2S$) calcd: C, 67.72; H, 4.90; Cu, 7.03; N, 4.65; O, 5.31; P, 6.85; S, 3.54. Found: C, 67.74; H, 4.92; Cu, 7.05; N, 4.63; O, 5.29; P, 6.85; S, 3.52.

*3.1.3. Crystal Structure Determinations of **15c** and **15f**.* The single-crystal X-ray diffraction study was carried out on the Bruker D8 Venture diffractometer with a PhotonII detector at 123(2) K or 298(2) K using Cu-Ka radiation (*l* = 1.54178 Å). Dual space methods (SHELXT)[35] were used for the structure solution, and refinement was carried out using the SHELXL-2014 (full-matrix least-squares on F^2).[36] Hydrogen atoms were refined using a riding model (H(N) for **15c** free). Semi-empirical absorption corrections were applied. Compound **15f** was refined as a twin with 2 domains; both *n*-propyl and one *n*-butyl moiety are disordered (see cif-file for details).

15c: colourless crystals, $C_{36}H_{28}N_3O_2PS$, M_r = 597.64, crystal size: 0.18 × 0.06 × 0.03 mm, triclinic, space group $P\bar{1}$ (no. 2), a = 9.4615(5) Å, b = 12.2923(6) Å, c = 14.1043(7) Å, α = 77.301(2)°, β = 70.645(2)°, γ = 74.755/2)°, V = 1477.26(13) Å^3, Z = 2, ρ = 1.344 Mg/m^{-3}, μ(Cu-K$_\alpha$) = 1.79 mm^{-1}, F(000) = 624, T = 123 K, $2\theta_{max}$ = 144.6°, 28,101 reflections, of which 5812 were independent (R_{int} = 0.025), 394 parameters, 2 restraints, R_1 = 0.031 (for 5558 $I > 2\sigma(I)$), wR_2 = 0.084 (all data), S = 1.05, largest diff. peak/hole = 0.47/−0.28 e Å^{-3}.

15f: colourless crystals, $C_{32}H_{28}N_3O_2PS{\cdot}C_{33}H_{30}N_3O_2PS$, M_r = 1113.23, crystal size: 0.18 × 0.12 × 0.03 mm, triclinic, space group $P\bar{1}$ (no. 2), a = 18.6988(5) Å, b = 18.8744(5) Å, c = 20.8063/6) Å, α = 103.938(2)°, β = 103.303(2)°, γ = 116.775(2)°, V = 5856.8(3) Å^3, Z = 4, ρ = 1.262 Mg/m^{-3}, μ(Cu K$_\alpha$) = 176 mm^{-1}, F(000) = 2336, T = 298 K, $2\theta_{max}$ = 144.6°, 96,411 collected data, merged to 23,046 unique reflections (using a HKLF5 file), 1411 parameters, 2775 restraints (see cif-file for details), R_1 = 0.065 (for 18,260 $I > 2\sigma(I)$), wR_2 = 0.211 (all data), S = 1.03, largest diff. peak/hole = 0.95/−0.47 e Å^{-3}.

CCDC 2182411 (**15c**) and 2182412 (**15f**) contain the supplementary crystallographic data for this paper. These data can be obtained free of charge from The Cambridge Crystallographic Data Centre via www.ccdc.cam.ac.uk/data_request/cif.

4. COMPUTATIONAL METHODS

4.1. Geometrical Optimization and Energy Calculations. Various quantum mechanical calculations were carried out to confirm the experimental results. The studied complexes were first optimized at the B3LYP/6-31G* level of theory.[37,38] The vibrational frequency and single-point energy calculations were performed upon the optimized geometries. All the adopted quantum mechanical calculations were executed at the B3LYP/6-31G* level of theory with the help of Gaussian 09 software.[39]

4.2. HS Analysis. In the current study, HS analysis[40] was executed to give an in-depth qualitative insight into the role of the main intermolecular interactions. Using HS analysis, the normalized contact distance (d_{norm}) surface was mapped over a fixed color scale ranging from red (−0.05 au) to blue (+0.75 au). The fingerprint plots were generated using the translated 1.0−2.8 Å range, and reciprocal contacts were considered. Moreover, the shape index and curvedness properties were mapped with the color range of −1.0 au (concave) to 1.0 au (convex) and a range of −4.0 au (flat) to 0.40 au (singular), respectively. The generated HSs and the associated 2D fingerprint plots were extracted using the CrystalExplorer17 software.[41]

5. CONCLUSION

New (*E*)-2-(1,4-dioxo-3-(triphenylphosphaneylidene)-3,4-dihydronaphthalen-ylidene)-*N*-substituted-hydrazine-1-carbothioamides were obtained during a one-pot reaction of 2,3-dichloro-1,4-naphthoquinone with thiosemicarbazides, triphenylphosphine (Ph_3P) in the presence of triethyl amine (Et_3N) as a catalyst. The reaction was a type of Eschenmoser nucleophilic addition. Utilizing the newly prepared ligands, their complexation with $CuCl_2$ and Ph_3P was investigated. Autoxidation occurs, and (*E*)-(2-(1,4-dioxo-3-(triphenyl-phosphaneylidene)-3,4-dihydronaphthalen-2(1*H*)-ylidene)-carbamothioyl)hydrazinyl)-((triphenylphosphanyl)oxy)copper

https://doi.org/10.1021/acsomega.2c04113
ACS Omega 2022, 7, 34463−34475

derivatives were formed in very good yields. Quantum mechanical calculations using the DFT method confirmed the stability of the obtained complexes..

■ ASSOCIATED CONTENT

Supporting Information

The Supporting Information is available free of charge at https://pubs.acs.org/doi/10.1021/acsomega.2c04113.

NMR (^{1}H NMR and ^{13}C NMR), IR, and mass spectra, in addition to HRMS spectra of compounds **15a-f** and **16a-f**; figures of UV Spectra of compounds **16a-f**; and X-ray figures and structural data and of compounds **15c** and **15f** (PDF)

■ AUTHOR INFORMATION

Corresponding Authors

Ashraf A. Aly − *Chemistry Department, Faculty of Science, Minia University, 61519 El-Minia, Egypt;* orcid.org/0000-0002-0314-3408; Email: ashrafaly63@yahoo.com, ashraf.shehata@mu.edu.eg

Stefan Bräse − *Institute of Organic Chemistry, Karlsruher Institut fur Technologie, 76131 Karlsruhe, Germany; Institute of Biological and Chemical Systems (IBCS-FMS), Karlsruhe Institute of Technology, 76344 Eggenstein-Leopoldshafen, Germany;* orcid.org/0000-0003-4845-3191; Email: braese@kit.edu

Authors

Mohammed B. Alshammari − *Chemistry Department, College of Sciences and Humanities, Prince Sattam Bin Abdulaziz University, Al-Kharij 11942, Saudi Arabia*

Martin Nieger − *Martin Nieger, Department of Chemistry, University of Helsinki, 00014 Helsinki, Finland*

Mahmoud A. A. Ibrahim − *Chemistry Department, Faculty of Science, Minia University, 61519 El-Minia, Egypt;* orcid.org/0000-0003-4819-2040

Lamiaa E. Abd El-Haleem − *Chemistry Department, Faculty of Science, Minia University, 61519 El-Minia, Egypt*

Complete contact information is available at: https://pubs.acs.org/10.1021/acsomega.2c04113

Author Contributions

CRediT authorship contribution statement. **Mohammed B. Alshammari:** editing and revision, **Ashraf A. Aly:** Conceptualization, writing, and editing, **Stefan Bräse**: Editing and revision. **Martin Nieger:** X-ray, Methodology, and editing, **Mahmoud A. A. Ibrahim**: Software, writing a draft, and editing. **Lamiaa E. Abd El-Haleem:** Conceptualization, writing, editing, methodology, and writing the draft.

Notes

The authors declare no competing financial interest.

■ ACKNOWLEDGMENTS

The authors thank the DFG-funded coordinative research center TR88/3MET, Karlsruhe Institute of Technology, Karlsruhe, Germany, for providing Prof A.A.A. with a two months project, enabling him to carry out analysis and facilities. We also acknowledge support from the KIT-Publication Fund of the Karlsruhe Institute of Technology.

■ REFERENCES

(1) Aithal, K. B.; Kumar, M. R. S.; Rao, B. N.; Udupa, N.; Rao, B. S. Juglone, a naphthoquinone from walnut, exerts cytotoxic and genotoxic effects against cultured melanoma tumor cells. *Cell Biol. Int.* **2009**, *33*, 1039−1049.

(2) Kosiha, A.; Parthiban, C.; Ciattini, S.; Chelazzi, L.; Elango, K. P. Metal complexes of naphthoquinone based ligand: synthesis, characterization, protein binding, DNA binding/cleavage and cytotoxicity studies. *J. Biomol. Struct. Dyn.* **2018**, *36*, 4170−4181.

(3) Geisler, H.; Westermayr, J.; Cseh, K.; Wenisch, D.; Fuchs, V.; Harringer, S.; Plutzar, S.; Gajic, N.; Hejl, M.; Jakupec, M. A.; Marquetand, P.; Kandioller, W. Tridentate 3-Substituted Naphthoquinone Ruthenium Arene Complexes: Synthesis, Characterization, Aqueous Behavior, and Theoretical and Biological Studies. *Inorg. Chem.* **2021**, *60*, 9805−9819.

(4) Zhivetyeva, S. I.; Zakharova, O. D.; Ovchinnikova, L. P.; Baev, D. S.; Bagryanskaya, I. Y.; Shteingarts, V. D.; Tolstikova, T. G.; Nevinsky, G. A.; Tretyakov, E. V. Phosphonium betaines derived from hexafluoro-1,4-naphthoquinone: Synthesis and cytotoxic and antioxidant activities. *J. Fluorine Chem.* **2016**, *192*, 68−77.

(5) Ramirez, F.; Dershowitz, S. The Structure of Quinone-Donor Adducts. I. The Action of Triphenylphosphine on *p*-Benzoquinone, 2,5-Dichloro-*p*-benzoquinone and Chloranil. *J. Am. Chem. Soc.* **1956**, *78*, 5614−5622.

(6) Loskustov, V. A.; Mamatyuk, V. I.; Beregovaya, I. V. The structure and properties of 3-(triphenylphosphoranylidene)-naphthalene-1,2,4(3*H*)-trione. *Russ. Chem. Bull.* **1999**, *48*, 371−374.

(7) Khasiyatullina, N. R.; Gubaidullin, A. T.; Shinkareva, A. M.; Islamov, D. R.; Mironov, V. F. New bisphosphonium salt containing a 1,4-dihydroxynaphthalene moiety: molecular and supramolecular structure. *Russ. Chem. Bull.* **2020**, *69*, 2140−2146.

(8) Huang, W.; Zhong, C.-H. Metal-Free Synthesis of Aryltriphenylphosphonium Bromides by the Reaction of Triphenylphosphine with Aryl Bromides in Refluxing Phenol. *ACS Omega* **2019**, *4*, 6690−6696.

(9) Khalafy, J.; Mohammadlou, M.; Mahmoody, M.; Salami, F.; Poursattar Marjani, A. P. Facile synthesis of new 10-substituted-5H-naphtho[1,2-e][1,2,4]triazolo[3,4-b][1,3,4]thiadiazin-5-ones. *Tetrahedron Lett.* **2015**, *56*, 1528−1530.

(10) Al-Alshaikh, M. A.; Lahsasni, S. A. Synthesis of Novel 2,3-Disubstituted 1,4-Naphthoquinone Derivatives Containing Indole, Quinoline, Thiazole and Imidazole Moieties. *Asian J. Chem.* **2013**, *25*, 10199.

(11) Forezi, L. da S. M.; Cardoso, M. F. C.; Costa, D. C. S.; Silva, F. de C. d.; Ferreira, V. F. 2,3-Dichloro-1,4-Naphthoquinone in Organic Synthesis: Recent Advances. *Mini-Rev. Org. Chem.* **2017**, *14*, 375−390.

(12) Aly, A. A.; Hassan, A. A.; AbdEl-latief, E.-S. S. M.; El-Sh, S. M. An Update of the Use of Thiocarbohydrazides and Thiosemicarbazides in the Preparation of Heterocycles and Their Biological Importance. *J. Heterocycl. Chem.* **2018**, *55*, 2196−2223.

(13) Choudhari, D.; Lande, D. N.; Chakravarty, D.; Gejji, S. P.; Das, P.; Pardesi, K. R.; Satpute, S.; Salunke-Gawali, S. Reactions of 2,3-dichloro-1,4-naphthoquinone with aminophenols: evidence for hydroxy benzophenoxazine intermediate and antibacterial activity. *J. Mol. Struct.* **2019**, *1176*, 194−206.

(14) Carroll, F. I.; Miller, H. W. The reaction of 2,3-dichloro-1,4-naphthoquinone with *p*-nitrobenzhydrazide. *Org. Prep. Proced.* **1970**, *2*, 259−263.

(15) Hergueta, A. R. Easy Removal of Triphenylphosphine Oxide from Reaction Mixtures by Precipitation with CaBr2. *Org. Process Res. Dev.* **2022**, *26*, 1845−1853.

(16) Wattanakanjana, Y.; Janwatthana, K.; Romyen, T.; Nimthong-Roldán, A. Crystal structures of copper(I) and silver(I) chloride complexes containing 4-phenylthiosemicarbazide and triphenylphosphine ligands. *ScienceAsia* **2021**, *47S*, 28.

(17) Gunasekaran, N.; Bhuvanesh, N. S. P.; Karvembu, R. Synthesis, characterization and catalytic oxidation property of copper(I)

complexes containing monodentate acylthiourea ligands and triphenylphosphine. *Polyhedron* **2017**, *122*, 39−45.
(18) Aly, A. A.; Abdallah, E. M.; Ahmed, S. A.; Rabee, M. M.; Abdelhafez, E. M. N. Metal complexes of thiosemicarbazones derived by 2-quinolones with Cu(I), Cu(II) and Ni(II); Identification by NMR, IR, ESI mass spectra and in silico approach as potential tools against SARS-CoV-2. *J. Mol. Struct.* **2022**, *1265*, 133480.
(19) Aly, A. A.; Bräse, S.; Weis, P. Tridentate and bidentate copper complexes of [2.2]paracyclophanyl-substituted thiosemicarbazones, thiocarbazones, hydrazones and thioureas. *J. Mol. Struct.* **2019**, *1178*, 311−326.
(20) White, A. R.; Multhaup, G.; Maher, F.; Bellingham, S.; Camakaris, J.; Zheng, H.; Bush, A. I.; Beyreuther, K.; Masters, C. L.; Cappai, R. The Alzheimer's Disease Amyloid Precursor Protein Modulates Copper-Induced Toxicity and Oxidative Stress in Primary Neuronal Cultures. *J. Neurosci.* **1999**, *19*, 9170−9179.
(21) Chen, X.; Zhang, X.; Chen, J.; Yang, Q.; Yang, L.; Xu, D.; Zhang, P.; Wang, X.; Liu, J. Hinokitiol copper complex inhibits proteasomal deubiquitination and induces paraptosis-like cell death in human cancer cells. *Eur. J. Pharmacol.* **2017**, *815*, 147.
(22) Sangeetha, S.; Murali, M. Non-covalent DNA binding, protein interaction, DNA cleavage and cytotoxicity of [Cu(quamol)Cl]·H2O. *Int. J. Biol. Macromol.* **2018**, *107*, 2501−2511.
(23) Hossain, G. M.; Abedin, M. d.; Bachar, S. C. Synthesis and Characterization of N1-Phenylhydrazine-1,2-bis(carbothioamide) and Its Evaluation for Antimicrobial, Antioxidant, and Brine Shrimp Lethality Bioassay. *Org. Chem. Int.* **2012**, *2012*, 278741.
(24) Baran, E. J. Structural Data and Vibrational Spectra of the Copper(II) Complex of L-Selenomethionine. *Z. Naturforsch.* **2005**, *60*, 663−666.
(25) Casper, J. M.; Remsen, E. E. Phosphoryl stretching frequencies of some tris para-substituted phenylphosphine oxides. *Spectrochim. Acta, Part A* **1978**, *34*, 1−4.
(26) Köhler, F. H. Paramagnetic Complexes in Solution: The NMR Approach. *eMagRes*; John Wiley & Sons, 2011.
(27) Drago, R. S. *Physical Methods in Chemistry*, 2nd ed; Saunders College Pub: Philadelphia, 1977.
(28) Gnangnon, B.; Baran, P. *Existence or Nonexistence of Cu(II) Complexes with Triphenylphosphine: Abstracts of Papers*; 247th ACS National Meeting & Exposition: Dallas, TX, United States, March 16-20, 2014.
(29) Bai, B.; Wang, W.; Wang, W.; Sun, S.; Chen, C. Triphenylphosphine as reducing agent for copper(II)-catalyzed AGET ATRP. *Chin. J. Polym. Sci.* **2015**, *33*, 1260−1270.
(30) Toshiyuki, S.; Yoshihiko, F.; Koichiro, S. Synthesis of Copper (I) triphenyl-phosphine complexes. *Chem. Lett.* **1972**, *1*, 163−164.
(31) Anitha, K.; Sivakumar, S.; Arulraj, R.; Rajkumar, K.; Kaur, M.; Jasinski, J. P. Synthesis, crystal structure, DFT calculations and Hirshfeld surface analysis of 3-butyl-2,6-bis(4-fluorophenyl)piperidin-4-one. *Acta Crystallogr., Sect. E: Crystallogr. Commun.* **2020**, *76*, 651−655.
(32) Arulraj, R.; Sivakumar, S.; Kaur, M.; Thiruvalluvar, A.; Jasinski, J. P. Crystal structures of three 3-chloro-3-methyl-2,6-diarylpiperidin-4-ones. *Acta Crystallogr., Sect. E: Crystallogr. Commun.* **2017**, *73*, 107−111.
(33) McKinnon, J. J.; Spackman, M. A.; Mitchell, A. S. Novel tools for visualizing and exploring intermolecular interactions in molecular crystals. *Acta Crystallogr., Sect. B: Struct. Sci.* **2004**, *60*, 627−668.
(34) McKinnon, J. J.; Jayatilaka, D.; Spackman, M. A. Towards quantitative analysis of intermolecular interactions with Hirshfeld surfaces. *Chem. Commun.* **2007**, *37*, 3814−3816.
(35) Sheldrick, G. M. SHELXT- Integrated space-group and crystal-structure determination. *Acta Crystallogr., Sect. A: Found. Adv.* **2015**, *71*, 3−8.
(36) Sheldrick, G. M. Crystal structure refinement withSHELXL. *Acta Crystallogr., Sect. C: Struct. Chem.* **2015**, *71*, 3−8.
(37) Becke, A. D. Density-functional exchange-energy approximation with correct asymptotic behavior. *Phys. Rev. A* **1988**, *38*, 3098−3100.
(38) Lee, C.; Yang, W.; Parr, R. G. Development of the Colle-Salvetti correlation-energy formula into a functional of the electron density. *Phys. Rev. B: Condens. Matter Mater. Phys.* **1988**, *37*, 785−789.
(39) Frisch, M. J.; Trucks, H. B.; Schlegel, H. B.; Scuseria, G. E.; Robb, M. A.; Cheeseman, J. R.; Scalmani, G.; Barone, V.; Mennucci, B.; Petersson, G. A.; Nakatsuji, H.; Caricato, M.; Li, X.; Hratchian, H. P.; Izmaylov, A. F.; Bloino, J.; Zheng, G.; Sonnenberg, J. L.; Hada, M.; Ehara, M.; Toyota, K.; Fukuda, R.; Hasegawa, J.; Ishida, M.; Nakajima, T.; Honda, Y.; Kitao, O.; Nakai, H.; Vreven, T.; Montgomery, J. A., Peralta, J. E.; Ogliaro, F.; Bearpark, M.; Heyd, J. J.; Brothers, E.; Kudin, K. N.; Staroverov, V. N.; Kobayashi, R.; Normand, J.; Raghavachari, K.; Rendell, A.; Burant, J. C.; Iyengar, S. S.; Tomasi, J.; Cossi, M.; Rega, N.; Millam, J. M.; Klene, M.; Knox, J. E.; Cross, J. B.; Bakken, V.; Adamo, C.; Jaramillo, J.; Gomperts, R.; Stratmann, R. E.; Yazyev, O.; Austin, A. J.; Cammi, R.; Pomelli, C.; Ochterski, J. W.; Martin, R. L.; Morokuma, K.; Zakrzewski, V. G.; Voth, G. A.; Salvador, P.; Dannenberg, J. J.; Dapprich, S.; Daniels, A. D.; Farkas, Ö.; Foresman, J. B.; Ortiz, J. V.; Cioslowski, J.; Fox, D. J. Gaussian 09, Revision E.01; Gaussian, Inc.: Wallingford CT, 2009.
(40) Spackman, M. A.; Jayatilaka, D. Hirshfeld surface analysis. *CrystEngComm* **2009**, *11*, 19−32.
(41) Turner, M. J.; McKinnon, J. J.; Wolff, S. K.; Grimwood, D. J.; Spackman, P. R.; Jayatilaka, D.; Spackman, M. A. *CrystalExplorer17*; University of Western Australia, 2017. http://hirshfeldsurface.net.

https://doi.org/10.1021/acsomega.2c04113
ACS Omega 2022, 7, 34463−34475